

THE URBAN HEAT ISLAND EFFECT OF AMSTERDAM: Observations and models in 2014 and Projections of the future urban climate. MSC thesis willem van der pas



Author W.W.J. (Willem) van der Pas

Study MSc Climate Studies

Chair group Meteorology and Air Quality, Wageningen University

WUR Registration number 900206-642-010

Examiner Prof. Dr. Bert Holtslag

Supervisors Dr. ir. Bert Heusinkveld, Reinder Ronda

Course code MAQ-80830

May 2015

## **TABLE OF CONTENTS**

Preface	p. 5
Acknowledgements	p. 5
Abstract	p. 7
1. Introduction	
	<u>р. 9</u> р. 9
1.1 Analysis of the Urban Heat Island of Amsterdam using weather observations	1
1.2 Modelling the Urban Heat Island of Amsterdam using the WRF model	p. 10
1.3 Calculating Urban temperatures using an existing Statistical relationship	р. 10 р. 11
1.4 The intensity of the Urban Heat Island of Amsterdam under a future climate	p. 11
2. Methodology	p. 13
2.1 Observation Analysis: Weather station setup and data collection	p. 13
2.2 WRF Modelling: model setup	р. 17
2.3 Statistical relationship: Derivation and parameters	p. 20
2.4 Future climate: Perturbation of the WRF model	p. 22
3. Results	p. 23
3.1 Observation Analysis	p. 23
3.2 WRF Modelling	p. 30
3.3 Statistical Relationship	p. 35
3.4 Future change	p. 39
4. Discussusion and Conclusion	p. 41
4.1 Observation Analysis	p. 41
4.2 WRF Modelling	р. 42
4.3 Statistical Relationship	p. 43
4.4 Future climate	p. 44
5. References	p. 45
6. Appendices	p. 47

### PREFACE

The Urban Heat Island effect (UHI) is an example of a meteorological phenomenon that affects human society. At the end of my BSc Soil, Water and Atmosphere I wrote my BSc thesis on the quantification of the UHI effect in the city of Utrecht, using data from amateur weather stations. In September 2013 I started my MSc Climate Studies, with focus on both the physical processes of climate change and the effect of a changing climate has on society. For my MSc thesis I wanted to conduct more research on the UHI effect in general and quantify future changes under different climate scenarios.

After establishing contact with Bert Heusinkveld and Reinder Ronda, I started working on the data

Willem van der Pas, May 2015

that was collected in the scope of the "Summer in the City" project from Wageningen University and the Netherlands eScience Center. For me, working with these large datasets has been an interesting endeavour and hopefully the WRF modelling performed in this research will contribute to the projects' ambition to make forecasts of human thermal comfort in urban areas.

It is expected that extreme temperatures will be more common in the future and that this will influence the intensity of the UHI effect. I think it is important to understand the changes that we can expect in the (near) future to mitigate this effect and ensure healthy living conditions for the population.

### **ACKNOWLEDGEMENTS**

I would like to acknowledge the following people or organizations for contributing to this research.

- Reinder Ronda, for his general guidance and sharing his knowledge of WRF.
- Bert Heusinkveld, for his general guidance and thoroughness regarding the data collection.
- Jisk Attema, for the assistance in the modelling part of this research.
- KNMI, providing the meteorological data at Schiphol.
- NCEP/NCAR, providing the reanalysis data used in WRF.
- Rijkswaterstaat, providing data on water temperatures near Amsterdam.
- Hobby meteorologist in Amsterdam, providing data of the weather station in Amsterdam Oud West. (http://www.weatherstationamsterdam.nl/)

### ABSTRACT

In 2014, 24 weather stations were installed in Amsterdam as part of the "Summer in the city" project from the Netherlands eScience Center to quantify the Urban Heat Island effect of the city. In June, July and August, an average UHI intensity of 0.67 °C was found, with extremes over 6 °C in the evening after hot summer days in July. The locations of the stations influence air temperature and provide an insight in the intra-urban intensity of the UHI. The weather stations that were used have been installed in the city of Wageningen before and those observations resulted in a statistical relationship for estimating urban temperatures. The performance of this original relationship in Amsterdam is good, but can be increased by implementing water temperature and surface water fraction in the equation. Using the WRF model with a high resolution domain of 100x100 metres, the urban temperatures over Amsterdam were modelled. The initial WRF run gave unsatisfying results after which the model setup was altered. These adaptations were successful in increasing the models' accuracy. Afterwards, the initial meteorological conditions were perturbed by adding 2.0 °C to all temperatures to simulate a warmer climate, such as the  $G_H$ -2050 scenario from KNMI. An average urban temperature increase of 1.78 °C is expected under such a climate after analysis of the WRF output.

### **1. INTRODUCTION**

Weather conditions in urban environments differ from those in rural areas. Higher temperatures, air pollution and lower wind speeds are often associated with these urban climates and these conditions can impact human health. The phenomenon where urban areas become warmer than their rural surroundings (Figure 1) is described as the Urban Heat Island (UHI) and has been subject of many scientific articles in the past. The amount of trees, building height, anthropogenic heat emissions, water availability, surface albedo and population size are all factors that affect the intensity of the UHI (Oke, 1973). The importance of a better understanding of the Urban Heat Island effect is increasing, because the part of the human population living in urban areas is increasing continuously and is projected to reach 60% in 2030, compared to 49% in 2005 (Golden, 2004).

Although cities in the Netherlands are generally small, research has shown that the UHI can be strong nonetheless, reaching 7-8 °C in certain urban areas (*Steeneveld et al., 2011*). The urban climate and UHI of Dutch cities have been examined in more detail, for example Rotterdam (*Heusinkveld et al., 2014*) Utrecht (*Brandsma, 2012*) and Wageningen (*Michiel van der Harst, Wageningen University, 2014*). For Amsterdam not even general research has been conducted yet, even though it forms with 1.5 million people the most populous urban agglomeration of the Netherlands. In 2014, Wageningen University started the "Summer in the City" project in cooperation with the Netherlands

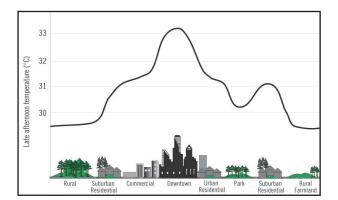


Figure 1: Temperatures in urban areas are higher than the rural surroundings, which is the Urban Heat Island effect. Image source: US EPA, 2008 (www.epa.gov)

eScience Centre and the project will focus in detail on the urban climate of Amsterdam and the impact on its inhabitants.

The research presented in this report is divided in four separate subjects: "Observation Analysis", "WRF Modelling", "Statistical Relationship" and "Future Climate" that will be introduced separately in the remainder of this chapter. Using these four subjects, we try to give better insight in the Urban Heat Island of Amsterdam and how it will develop under a future climate. Using observations, numerical weather models and statistical analysis we aim to better understand how land use, weather and local environment affect the urban temperatures and therefore the quality of life of the people living in the city. Each of the chapters in the report is divided in four parts, corresponding to the four main subjects of this research. In chapter 2, the methodology of the research is described and chapter 3 presents the results. Conclusions are drawn and discussed in chapter 4. Finally, a list of used references is presented in chapter 5. The appendices contain many details, graphs and photos that were used in this research, but not contribute to the clarity of the report directly.

#### 1.1 ANALYSIS OF THE URBAN HEAT ISLAND OF AMSTERDAM USING WEATHER OBSERVATIONS

Many cities throughout the world have been subject to UHI research before and there are numerous methods of assessing the urban temperature. Examples of such methods range from combining GIS and the analysis of satellite images (Lo et al., 1997; Voogt & Oke 2003; Chen et al., 2006; Streutker, 2003) to the use of amateur weather observations (Steeneveld et al., 2011) and cycling transects through the city with a sensor-equipped cargo bicycle (Heusinkveld et al., 2010). The UHI is typically defined as the difference between the rural and urban temperatures and can be calculated using synchronised measurements. A number of small weather stations is installed in a city for a certain period and then compared with a nearby rural reference station. Similar measuring campaigns have

been performed in cities all over the world, ranging from the metropolitan city of London in the midlatitudes (*Watkins et al., 2002*), the Australian city of Melbourne (*Morris et al., 2001*) and the high latitude city of Fairbanks, Alaska (*Magee et al., 1999*).

In the first part of this MSc thesis report, an analysis of the UHI of Amsterdam is performed using 24 weather stations that are installed at different locations in the city. These stations have operated in Wageningen since August 2013 and provided data to help understand the UHI of this city (Michiel van der Harst, Wageningen University, 2014). The use of many identical automated weather stations is unique in the field of urban meteorology research. With this number of weather stations, there is one measurement per  $\sim$ 4 km<sup>2</sup> for the city of Amsterdam. While the UHI effect can vary a lot within such area, this measuring density is still relatively high compared to other UHI research. For example, the 68 stations that were installed during a field campaign in London resulted in 1 measurement per ~14 km<sup>2</sup> (Watkins et al., 2002).

The old city centre of Amsterdam contains many old buildings and has been appointed as a UNESCO world heritage site for the unique seventeenth century city canal ring ('grachten'). Counterintuitively, these water bodies might increase the maximum intensity of the UHI in summer time (*Heusinkveld et al., 2014, Steeneveld et al., 2013*). Areas in Amsterdam where little surface water is present can be found in the suburban areas Bijlmer, Diemen and Osdorp.

#### **Research questions:**

- Are the 24 installed weather stations useful to find an UHI effect in the city of Amsterdam?

- What is the intensity of this UHI effect and under what meteorological conditions is it the strongest?

- Can we quantify an intra-urban UHI and can this be related to differences in local urban environment such as surface water?

#### 1.2 MODELLING THE URBAN HEAT ISLAND OF AMSTERDAM USING THE WRF MODEL

The next section of the report will focus on modelling the UHI with the Weather Research and Forecasting model (WRF) to see if the urban climate of Amsterdam can be forecasted at street level, and how the model relates to our observations. The WRF model is a mesoscale meteorological model that is often used for research on mesoscale meteorological phenomena near the surface, such as the Urban Heat Island effect (Mirzaei & Haghighat, 2010; Yang et al., 2012; Chen et al., 2011). The finest grid of the model will have a high spatial resolution (100x100 metres) to be able to give predictions at street resolution. With more insight in the UHI of Amsterdam and a satisfying model, weather predictions can be made on a small spatial scale. These predictions can be used to provide useful information on the temperature to the people depending on their location, rather than that of a rural reference station. For the summer of 2015, the WRF model will be used by the Netherlands eScience Centre to forecast the Amsterdam UHI effect with similar model settings for the first time.

#### **Research questions:**

- Can WRF accurately model the temperatures observed at the weather stations?

- (How) can the model be improved to better match the observations?

#### 1.3 CALCULATING URBAN TEMPERATURES USING AN EXISTING STATISTICAL RELATIONSHIP

Statistical analyses were performed on the dataset, following the MSc thesis of Michiel van der Harst (*Wageningen University, 2014*). In his report, he presents several formulas for relating temperatures in the city of Wageningen during the summer of 2013 to other parameters such as NDVI, soil moisture, rural temperature and radiation. The calculation for the hourly urban temperature at a station was constructed from 1513 hourly observations and tested for seventeen independent variables. The resulting relationship for Wageningen is:

$T_{urk}$	an =	0.9765	*	T <sub>rural</sub> -	0.	8204	*
log	(U)	- 0.0231	L2	* API	- 2	.365	*
NDV	'I +	2.392e <sup>-08</sup>	*	Rad	, <b>+</b>	2.70	6

Where  ${\tt T}_{\tt rural}$  is the temperature at a reference station. The other four terms (U, API, NDVI, Rad<sub>urban</sub>) are variations of wind speed, soil moisture, vegetation and radiation respectively. The exact description of these terms are elaborated in section 2.3. The statistical parameters of this model all indicate a high performance of the model for Wageningen ( $R^2$  > 0.97 and RMSE < 0.88 °C). However, this relationship has been tested for Rotterdam city as well by another MSc student with results that show that these kind of statistical relations are possible only useful for the city that they are derived for (Bart Limbeek, Wageningen University, 2015). This research will test the model using observations in Amsterdam in the summer of 2014 (June, July and August), and will also be compared to the WRF model output to find which method performs better during a warm period.

#### **Research questions:**

- Can the statistical relationship that was derived for Wageningen predict urban temperatures in Amsterdam?

- When does the relationship perform best, and under what conditions does it fail?

#### 1.4 THE INTENSITY OF THE URBAN HEAT ISLAND OF AMSTERDAM UNDER A FUTURE CLIMATE

By analysing the observations and two modelling methods, we will gain understanding of the present Urban Heat Island effect of Amsterdam. However, the rate of climate change due to anthropogenic emissions of carbon dioxide in the past century has been alarming, and is not expected to slow down. For this reason, the Royal Netherlands Meteorological Institute (KNMI) has prepared future climate scenarios that can occur in the Netherlands. In the most recent version of these scenarios the number of days with a maximum temperature above 25 °C is expected to increase by 22% to 70% in 2050 depending on the scenario (*KNMI*, 2014). The KNMI scenarios are derived from the IPCC climate scenarios, and apply for the Netherlands specifically. The scenarios consist of 4 different types of climate variations ( $G_L G_H W_L W_H$ ). The G-scenarios represent a mild global temperature increase (+1 °C in 2050 and +1.5 °C in 2085 relative to 1981-2010), whereas the W-scenarios indicate a higher global temperature increase (+2 °C in 2050 and +3.5 °C in 2085 compared to 1981-2010). The L and H subscripts indicate if changing global weather patterns result in more westerly flows in the Netherlands (H-scenarios) or that it remains stable (L-scenarios).

After the massive heat wave in Europe in 2003, many research focussed on the relation between the urban climate and mortality rates. Estimations of the additional mortality in Europe due to this heat wave are as high as 70000 people (Robine et al., 2007). The ongoing urbanization and climate change are likely to contribute to the threat on public health (Luber & McGeehin, 2008). Already 53% of the world population lives in an urban environment (3.8 billion people), and this number is expected to rise to 60% in 2030 (5.0 billion people), (Population Reference Bureau, 2014). Many cities will have over one million inhabitants. It is essential to understand the evolution of a city's Urban Heat Island under these changing conditions. The final part of this thesis report will focus on the development of the UHI of Amsterdam under these future climate scenarios. One way to model the intensity of the Urban Heat Island of Amsterdam under a future climate scenario, is to perturb the input data of the WRF model (Doherty et al., 2009). Since computing time is costly and timeconsuming, only one WRF run with altered climate will be performed. Following similar research the chosen temperature perturbation for the model is 2.0 °C for technical reasons (Attema & Lenderink, 2011). This perturbation is similar to the KNMI scenarios G<sub>H</sub>-2050 and W<sub>1</sub>-2085.

#### **Research questions:**

- Can we predict how the UHI effect will change under a future climate using WRF?

- If so, how large will this change be and what will be the impact on the UHI frequency/intensity.

### 2. METHODOLOGY

This report relies heavily on data collection in Amsterdam and data from WRF model output. Analyses are mostly performed in Microsoft Excel and MATLAB R2013a. Google Earth has been a valuable tool for maps and spatial data visualization.

#### 2.1 OBSERVATION ANALYSIS: WEATHER STATION SETUP AND DATA COLLECTION

In May 2014, 24 identical weather stations at different locations in the city of Amsterdam were installed. These stations were already used in meteorological research in Wageningen and have been used in the MSc thesis report of Michiel van der Harst (*Wageningen University, 2014*). The locations of the stations in Amsterdam can be found in the map displayed in Figure 2. In Appendix A, a detailed description of each station and its surroundings is given.

The stations were mounted to lamp posts or other available poles in different locations in Amsterdam. The stations consist of a VP-3 Humidity/Temperature sensor from Decagon Devices with resolutions of 0.1 °C and 0.1% respectively. The sensor is covered by a 184 millimetres cylindrical shield. On top of this shield, two small solar panels are mounted that power a ventilation fan from Davis Instruments. Data is averaged every five minutes and stored on Em50G data loggers from Decagon Devices. Using a GPRS network, this data is automatically uploaded six times per day, greatly reducing the amount of field work (i.e. manual data collection). An example of the installation of a station can be found in Figure 2 and technical specifications of the equipment in Appendix B.



Figure 2: Satellite picture of Amsterdam with the 24 installed weather stations marked using a white pointer. The yellow pointer marks reference station Schiphol Airport.



Figure 3 Setup of a weather station as used in this research. Wind measurements are performed in the cylinder on top, temperature and humidity is measured in the larger cylinder below the solar panel. a datalogger is attached to the pole on the left.

Initially all data loggers operated in local time (UTC+2). Unfortunately, during maintenance or manual data collections at the stations time stamps were sometimes perturbed to UTC. Using field logs and 2 distinctive weather events the data could be synchronized again. One such weather event was the passage of a cold front on October 7<sup>th</sup> when temperature drops of 1 degree in 5 minutes were measured at the stations. More details of this data synchronisation can be found in Appendix C.

To quantify the intensity of the Urban Heat Island, a rural reference station is needed. In this report, the official weather station of the Royal Dutch Meteorological Institute (KNMI) at Schiphol was used as a background station. The station is equipped with many sensors and data is publicly available online in hourly and daily format. The location of this station is approximately 10 kilometres to the South-West of the centre of Amsterdam, and can be found in Figure 2 as well. After collection, all data is synchronised and converted to UTC, local time is +2h in summer time and +1h in winter time (winter time started at 26<sup>th</sup> of October 01:00 UTC). MATLAB was used to plot spatial maps of the UHI intensity at different times and the characteristics of the stations can be given by numbers and statistics. No temperature correction has been made for altitude differences between stations since the city of Amsterdam is quite flat and street elevations of the measurement locations are all between -3m and +3m above sea level.

On October 17<sup>th</sup> 2014, five of the stations were equipped with a DS-2 sonic anemometer from Decagon Devices. This sensor has a threshold of 0.00 m/s in measuring wind speeds and a very high resolution of 0.01 m/s. It averages data on wind speed and direction every five minutes. The locations were selected because of their interesting local urban environment; #Ams3 and #Ams7 are located in typical 'street canyons' whereas #Ams2 and #Ams16 are in busy streets in the centre near a city canal. #Ams25 is a station located between tall commercial buildings. On November 1<sup>st</sup> station #Ams8 on the small island in het IJ was equipped with such a sensor as well resulting in six location where wind is measured. The lack of wind data in the summer of 2014 is unfortunate, since the data could have been used in analysing the output of the WRF model that covers 4 hot days in July in which the highest UHI intensities were measured. However, using the amateur meteorologists' network www. wunderground.com, one 'amateur weather station' was selected in Amsterdam. The use of amateur weather stations has been proven valuable in other UHI research in the Netherlands. (Steeneveld et al., 2011). This station has data available for the whole year and its location (N 52.361672, E 4.863245) is close to one of our stations #Ams13 (about 350 metres apart). The equipment used is Vantage Pro2 UV/Solar from Davis Instruments and installed on a rooftop near a street canyon, as presented in Figure 4. Wind and temperature data from this station will be validated with our own observations first.

The Sky View Factor (SVF) can be a useful indicator for predicting the UHI (Gal et al., 2009), since long wave radiation from urban surfaces will radiate less towards the open sky in areas with low SVF numbers and thus have less possibilities of cooling the city. The SVF is calculated from the fraction of sky that is visible from a location. In a wide open field, this number will be close to 1, while in a street with tall buildings or high amounts of tree coverage, the number will be closer to 0. For each of the measuring locations the SVF is determined by analysing fish eye photographs. The lens that was used is a 4.5mm F2.8 EX DC Circular Fisheye HSM from Sigma. The photographs were made in a short period, to ensure the same amount of tree foliage (October 8th - October 23<sup>rd</sup>). When shooting the photos, the camera was not positioned directly below the lamp posts with the stations attached but more towards the middle of the street. The lamp posts often were close to the buildings, which would result in lower SVF values

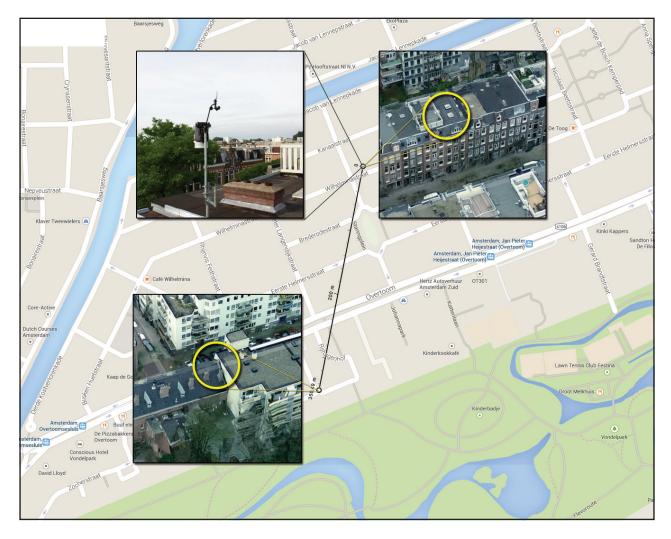


Figure 4: Amateur weather station located on a roof in Amsterdam (top left) and the location of that station (top right). Bottom left is the location of station #Ams13.

than we would find in the majority of the street.

Using Adobe Photoshop CS6, the sky view photos were aligned and transformed into a monochromatic format that can be imported by the Rayman 2.0 software (*Matzakaris et al., 2010*), to calculate a value for SVF. Rayman 2.0 was also used to calculate hourly time series of incoming shortwave radiation per station from this photo, depending on solar altitude and obstructions by buildings. The software does not take into account any cloud coverage, but gives the maximum possible amount of radiation instead. Measurements of sunshine duration per hour at Schiphol were used to correct for this.

The original photos were transformed with Photoshop CS6 to the panoramic views in the appendices, which give better insight in the immediate surroundings of the weather station. In Figure 5 below, an example of a photograph and its transformations is presented.



Figure 5: Original fish eye photograph of station #Ams4 (Top left), the transformation used to calculate Sky view factor and incoming solar radiation (top right) and a panoramic transformation (bottom).

#### 2.2 WRF MODELLING: MODEL SETUP

Two runs were performed for this part of the research using WRF version V3.5.1. The aim of the first WRF run was to find if the model can accurately model the urban temperatures at a high resolution during a few hot days. The 18<sup>th</sup> and 19<sup>th</sup> of July were selected, since these days large UHI intensities in the evening and night were observed. Because the model needs a start-up period, the modelled time period in WRF run 1 is from 17-07-2014-00:00:00 – 20-07-2014-00:00:00. The model uses a time step of 60 seconds. Meteorological NCEP FNL reanalysis data at 1 degree resolution was acquired from the National Centre of Atmospheric Research (*NCEP/NCAR, 2014*).

For WRF run 1, four nested domains were setup with increasing resolution (Table 1). The fourth and final domain covers the entire city of Amsterdam in a grid cell resolution of 100x100 metres. All the observation stations lie within the range of this domain, including reference station Schiphol. For the Improved run, an additional high resolution domain was added which contains the city of Wageningen. The results from this domain will not be discussed in this research, but will be analysed in the greater scope of the Summer in the City project. The domain with Amsterdam did not increase in grid size or position so comparison between the two runs is possible. The domain setup for the Improved run can be found in Table 2 and Figure 6 below. After viewing the results of the Initial

Table 1: Domain configuration	for WRF run 1.
-------------------------------	----------------

Domain	Grid cells	Cell dimensions (m)	Domain dimensions (m)
d01 (North west Europe)	120 x 120	12500 x 12500	1500000 x 1500000
d02 (Netherlands)	121 x 121	2500 x 2500	302500 x 302500
d03 (North Holland province)	121 x 121	500 x 500	60500 x 60500
d04 (Amsterdam)	136 x 176	100 x 100	13600 x 17600

Table 2: Domain configuration for WRF run 2. Domain 1 and 2 are identical to the first WRF run.

Domain	Grid cells	Cell dimensions (m)	Domain dimensions (m)
d03 (Central Netherlands)	226 x 206	500 x 500	113000 x 103000
d04 (Wageningen)	121 x 121	100 x 100	12100 x 12100
d05 (Amsterdam)	136 x 176	100 x 100	13600 x 17600

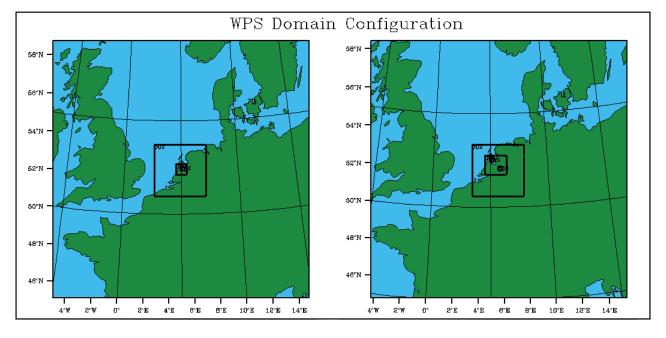


Figure 6: Domain configuration for WRF run 1 (left) and WRF run 2 and 3 (right).

p. 17

run, an additional day of start-up was implemented to ensure proper heating of the buildings and urban environment. This increased the modelled period with 24 hours to 16-07-2014-00:00:00 – 20-07-2014-00:00:00.

Land use maps are based on TOP10NL from the Dutch Kadaster and adapted by WUR/Netherlands eScience Centre (private communication, for details see: www.met.wau.nl/SummerInTheCity). Figure 7 below shows the final land use map of fourth domain with each of the station locations. The domain of Amsterdam is identical for both WRF runs, so this figure is valid for both runs.

The Unified Noah land-surface model is used in all domains, and the Revised MM5 Monin-Obukhov scheme (Jimenez) is used for the surface layer. When modelling the PBL there are several PBL schemes available in WRF. In this research the Yonsei University boundary layer scheme is used (YSU, Hong et al., 2006). It is an updated version of the Medium Range Forecast (*MRF, Hong and Pan,* 1996) PBL scheme that uses nonlocal closure and has proven its use in UHI boundary layer research before (*Lin et al., 2008*). The fourth domain does not use a PBL scheme because the scale of typical boundary layer phenomena are larger than the grid cells of this domain. The Smagorinsky turbulence closure is used in this domain instead.

The Grell-Freitas cumulus parametrization is used in the large domains d01 and d02 and has been disabled in domains d03 and d04. For a better representation of momentum, heat exchange and humidity in an urban environment it is important to implement an Urban Canopy Model (UCM). It improves the accuracy of the lower boundary conditions in urban

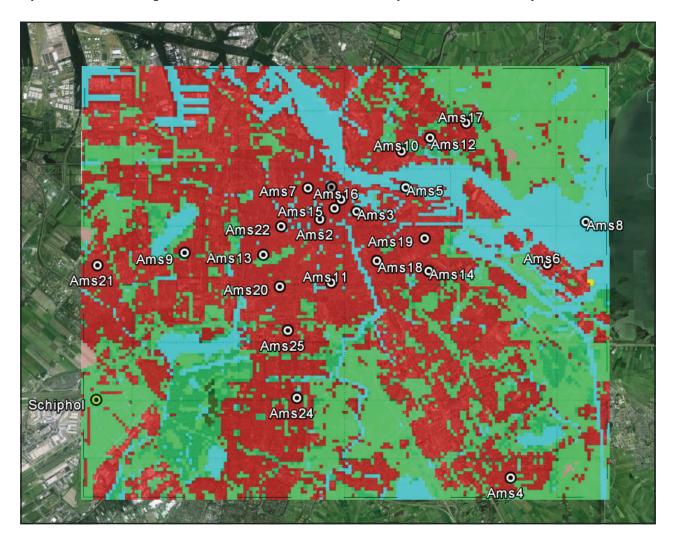


Figure 7: Amateur weather station located on a roof in Amsterdam (top left) and the location of that station (top right). Bottom left is the location of station #Ams13.

environments (cities). In this research the single-layer UCM was used, which uses many city parameters such as building height, incoming radiation, the heat capacity of the surface layers and buildings, road width, amount of vegetation to calculate the

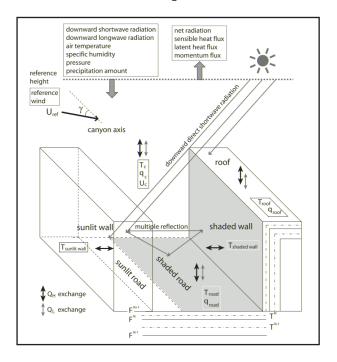


Figure 8: Visual representation of the single-layer urban canopy model (UCM). Source: Ryu, Y. H., Baik, J. J., & Lee, S. H. (2011).

urban temperature. In this UCM, the street canyon is represented by a single layer with different surfaces (walls, road and roofs) and takes into account the physical interactions between them for radiation, wind or heat exchange as can be found in Figure 8 (*Touchaei & Akbari, 2013*).

For shortwave and longwave radiation, the Dudhia and rttm scheme are used repectively for d04. The other domains use the rttmg scheme for both radiation types.

The Initial run used a water temperature for lakes and rivers that was extrapolated from nearby sea surface temperature points. However, it is assumed that water temperatures in the shallow city canals and het IJ are higher than that of the North Sea. In the Improved run, water temperatures have been set manually. For this, data on water temperatures at four different locations in Amsterdam have been obtained from Rijkswaterstaat. The measurement locations can be found in Figure 9. From this figure, it also follows that temperature differences between the four different locations are small. The water temperature that was used in the Improved run is

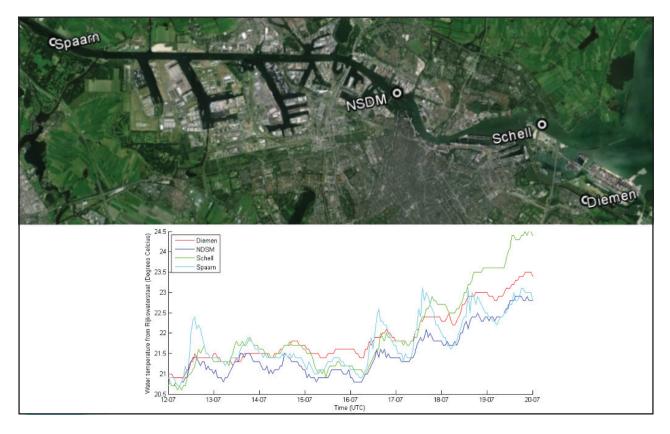


Figure 9: Rijkswaterstaat measurement sites of water temperature (top), and the measured water temperature at those station during a warm summer period (bottom).

21.24 °C and was constructed from the average water temperature of the 15th of July, and averaged over the four locations as well to come up with one value for the entire city.

#### 2.3 STATISTICAL RELATIONSHIP: DERIVATION AND PARAMETERS

Since the relationship is originally derived for summer months in Wageningen, it will be tested only for the months June, July and August. After data collection, the urban temperature can be calculated for each hour, at each station using the following equation derived in previous research (van der Harst, 2014):

 $T_{urban} = 0.9765 * T_{rural} - 0.8204 *$ log (U) - 0.02312 \* API - 2.365 \* NDVI + 2.392e<sup>-08</sup> \* Rad<sub>urban</sub> + 2.706

where  $T_{rural}$  is the temperature at the rural reference station. For this research, Schiphol was chosen as reference station. The negative effect of wind on the UHI is implemented by taking the logarithm of the average horizontal wind at 2 meters. The wind speeds used in this formula are those observed at Schiphol since no wind data was available for the JJA period at the stations. Rad<sub>urban</sub> is the sum of incoming solar radiation of the past 16 hours at Schiphol, and corrected for obstructions by implementing the SVF photographs. The Antecedent Precipitation Index (API) is an index used for estimating soil moisture and is a summation of previous precipitation multiplied with a regression coefficient:

$$API_{t} = k * API(_{t-1}) + P(_{t-1})$$

For Wageningen, it was found that a regression coefficient of k=0.95 fits to soil moisture measurements well. Unfortunately there were no actual soil moisture measurements available for Amsterdam, and implementing the same formula with rain data from Schiphol resulted in unrealistically high API values. By decreasing the regression coefficient to k=0.90 and implementing a precipitation maximum of 10 mm per day, the API values fit in a more realistic range. It is assumed that if there is more than 10 mm of rain per day, this surplus would runoff the surface rather than infiltrate the soil. The API for Amsterdam was calculated from April onwards to ensure reasonable values at the beginning of the observation period.

The NDVI is the Normalized Difference Vegetation Index, used to assess the amount of "greenness", i.e. the amount of vegetation that is actively photosynthesizing and adds to the evapotranspiration. It is calculated from remote sensing images with a spatial resolution of 25 meters using the following formula:

NDVI = (NIR - VIS) / (NIR + VIS)

where NIR is the reflectance in the near-infrared light (from 0.7 to 1.1  $\mu$ m) and VIS the reflectance in the visible light range (from 0.4 to 0.7  $\mu$ m).

NDVI values during the summer were taken from the website www.groenmonitor.nl for each station in Amsterdam. Depending on cloud coverage, between 9 and 13 satellite images are available in this period for each station. The values in a 100 meter radius around the station were averaged and linearly interpolated to construct values for each day of the JJA period. A radius of 100 meter was used to obtain a reliable average that can be compared with the WRF grid cells later on. Average summer values can be found in the station descriptions in the appendix. The final variable is  $\operatorname{Rad}_{\operatorname{urban}}$ , which is the sum of the incoming shortwave radiation of the past 16 hours. This radiation is calculated by Rayman 2.0 and depends on the sky view factor, as described previously in section 2.1.

After analysis of the original calculation, a first attempt to derive a similar relationship for Amsterdam will be performed. In the scope of this research it was not feasible to test all seventeen variables that were used to derive the equation for Wageningen, therefore only the original five independent variables will be considered, along with water temperature and surface water fraction. The water temperature is calculated by averaging the water temperatures measured at the four locations from Rijkswaterstaat as described in section 2.2, which results in hourly values. The fraction of surface water is calculated by simply counting the number of grid cells with water as land use that surround the station. For this calculation, a radius of 300 metres was used. In Figure 10, the water fraction is visually presented. The black circles are the locations of the stations, from which the fraction of surface water is adopted. The values can be found in Appendix A for each station. Following the methodology for the derivation in Wageningen a filter was applied on the data to remove observations at times where the Urban Heat Island intensity is expected to be low. If the precipitation sum of the past 16 hours at Schiphol exceeded 3 mm, these observations were filtered out. Similarly, fog was eliminated from the observations if the visibility at Schiphol was measured to be lower than 1000 metres somewhere in the past 16 hours. Out of 2208 hourly observations, 1674 hours remained.

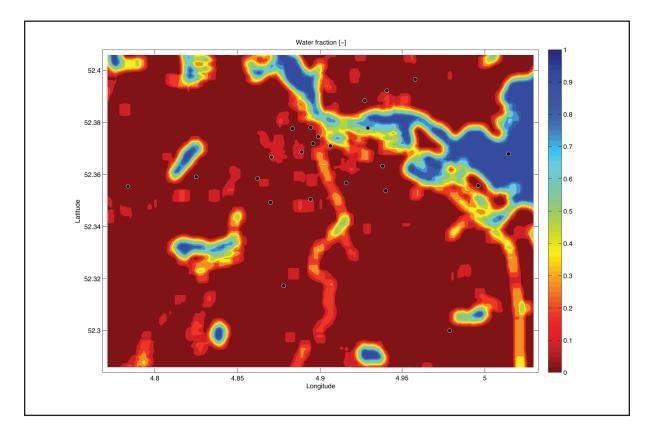


Figure 10: Water fraction calculated from land use maps. Black markers indicate locations of weather stations.

# 2.4 FUTURE CLIMATE: PERTURBATION OF THE WRF MODEL

A third WRF run was performed to find the effects of a warmer climate on the UHI intensity of Amsterdam. The domain setup is similar as in WRF run 2 and can be found in Table 2 and Figure 6, but without the high resolution domain for Wageningen. The third domain is kept constant to make sure that the boundary conditions for the Amsterdam domain are similar. WRF domains do not interact with higher domains, so the exclusion of the Wageningen domain will not have influence on the model output. Model run time is kept constant, as well as all parametrization schemes.

All air temperatures in the NCEP FNL reanalysis data were perturbed by +2.0 °C. This results in a shift of the entire vertical temperature profile as can be seen in Figure 11. In the WRF post-processing program WPS, original soil and water temperatures in were increased with 2 degrees for each domain and all depths. This way, we have implemented a warmer climate that corresponds to the WL scenario for 2050 from the KNMI.

Like in the article of Attema, it is assumed that the relative humidity does not change in the future climate scenario, which is proven to be a reasonable assumption (Willett et al., 2010). For the sake of simplicity, more assumptions were made on the initial conditions. Although the land use of the old city centre is not expected to change much due to its monumental heritage, it is also assumed that the land use of the entire city will not change either. In reality, the city will probably expand in the coming decades, increasing the area of paved surface and thereby decreasing evaporation possibilities. Also, even though population will probably grow, we assume that the same number of people will reside in the streets. Anthropogenic heat will be kept constant, even though a different climate could indicate an increased need for air conditioning or otherwise influence human energy consumption.

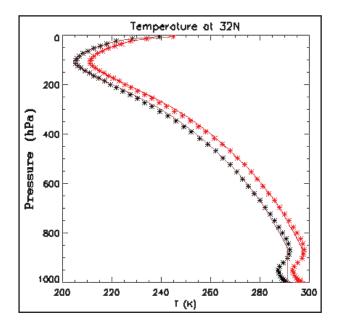


Figure 11: Example of the shift of the vertical temperature profile in the third WRF run to simulate a warmer climate. The red line indicates the perturbed temperature profile.

#### **3.1 OBSERVATION ANALYSIS**

The 24 weather stations were installed at the end of May 2014. As a first analysis we observe the three summer months June, July and August. Later on there will be focus on several shorter time series that are of particular interest. The selected days will act as case studies in the modelling part later on. Unfortunately, station #Ams25 did not record well and only started recording data from October 17th 2014 onwards. This station is therefore not taken into account in this analysis. All time notations in the analysis are in UTC, local time is +1 hour, and daylight saving time is +1 hour from March until 26th of October. In the following figures white dots represent the measuring stations, with reference station Schiphol being the station in the bottom left corner. More detailed statistics of observations per station can be found in the appendices.

In Figure 12, it can be observed that the city is warmer than its surroundings. The average temperature at Schiphol over the entire period is the lowest observed with 17.3 °C. All stations in the city show a higher average temperature, ranging from 17.4 °C (station #Ams10) to 18.4 °C (station #Ams15). The five stations with the highest average temperatures all lie within one square kilometre around the Dam Square in the city centre, as can be observed in Figure 13 where the previous plot is plotted on top of a satellite image of Amsterdam. This can be considered as the 'thermal core' of Amsterdam.

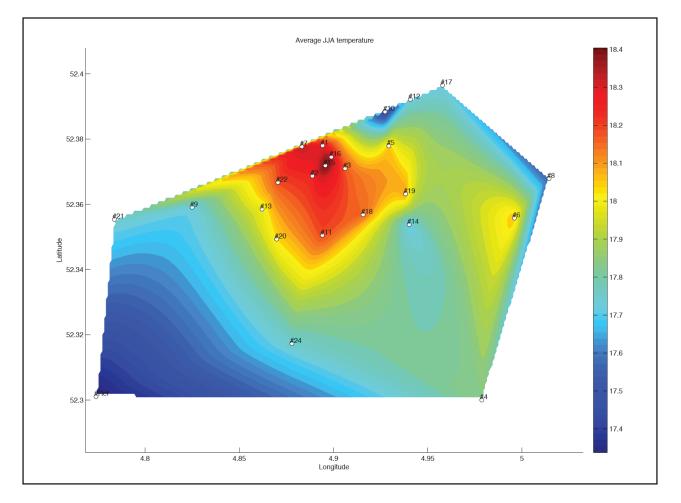


Figure 12: Average temperature recorded at the stations (white markers) for June, July and August combined.

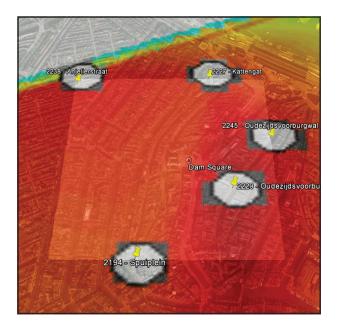


Figure 13: Impression of the 'thermal core' of Amsterdam by overlaying Figure 12 on a satellite image. The five stations that record the highest average JJA temperature are located within the white square (1 x 1 km) with the Dam Square in the centre of it.

The intensity of the Urban Heat Island (UHI) is defined as the temperature difference between the measurement stations and Schiphol at that particular hour. In Figure 14 the average UHI intensity per station is plotted for the entire summer period. Since Schiphol is the reference station, its UHI is zero by definition. The spatial pattern that emerges in the figure is of course similar to figure with the average temperatures, but of different intensity. The UHI (at time h in UTC) is defined in the following equation:

Positive values for the UHI intensity are thus associated with higher temperatures in the city. The average summer UHI intensities for the city stations range from 0.12 °C to 1.11 °C, and a station-wide average over the summer period results in an average UHI intensity of 0.67 °C. This is lower than other Dutch cities where median UHI's up to 3.0 °C have been found (*Steeneveld et al., 2011*). The average

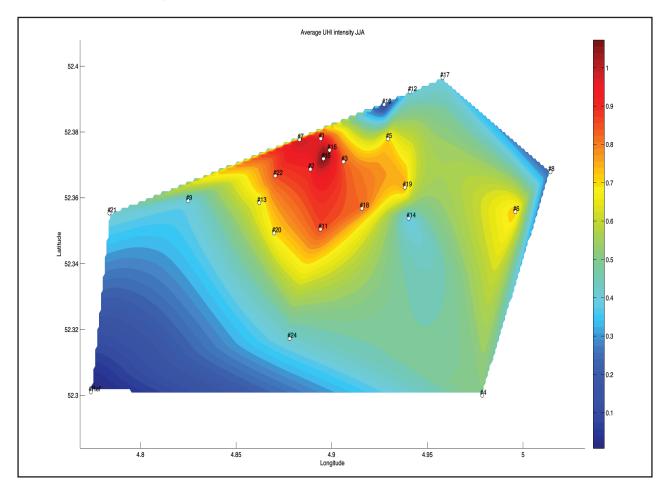


Figure 14: Average Urban Heat Island recorded at the stations (white markers) for June, July and August combined. Reference station Schiphol is the bottom left marker, where the UHI is 0 degrees by definition.

daily maximum UHI of Amsterdam is 2.54 °C, and is calculated by averaging the largest temperature difference of each station and Schiphol, per day (24 hours).

The increased temperature in the city results in lower values for relative humidity at those places, as can be observed in Figure 15. This difference in humidity however, is not only due to higher temperatures: if we combine temperature and humidity measurements to calculate the dew point temperature using the August-Roche-Magnus (*Lawrence, 2005*) formula we find that some stations do record lower average dew point temperatures than others. The relative humidity measured at reference station Schiphol is the highest at 78.1%, but its average dew point temperature (11.91 °C) is surpassed by three stations on the edge of the city (#Ams4, #Ams16, #Ams17). In general, humidities in the city centre are lower than in the surrounding grasslands.

The intensity of the UHI effect shows large variation in time due to meteorological conditions such as high pressure systems or high wind speeds. Variation in space, however, can also be explained by the different built surface characteristics of the stations. This intra-urban variation of UHI depends on many urban parameters such as building height and street width, evapotranspiration by vegetation or water and anthropogenic heat. For example, the most eastern station, #Ams8 is situated on a small island in het IJ. No buildings are present and the sky view factor is therefore 1.0. Open water is omnipresent and acts as an 'air conditioning system' for this station as can be seen in Figure 16. If the reference temperature is below ca. 19 °C the UHI intensity at the station is generally positive. If air temperatures at Schiphol are higher than this threshold, the water acts as a cooling system and a negative UHI effect is observed. The threshold temperature is closely related to the water temperature. The average water temperature at the four RWS locations is 20.39 °C over the JJA period. It is assumed that the graph will change depending on the months or seasons that are observed. Logically, in winter time water temperatures will be much lower than in the period observed in this research.

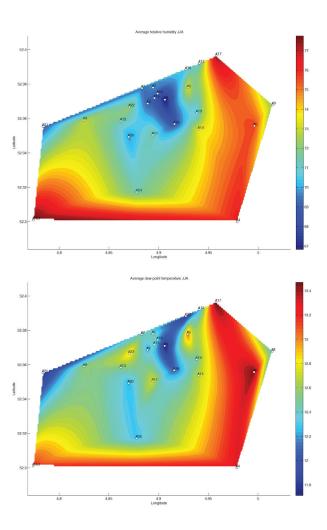


Figure 15: Average relative humidity recorded at the stations (white markers) for June, July and August combined (top) and average dew point temperature (bottom).

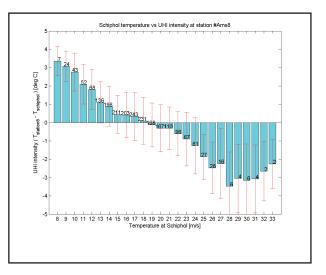


Figure 16: the intensity of the Urban Heat Island effect at station #Ams8, depending on the temperature at reference station Schiphol.

For station #Ams8, a similar pattern is observed if the global radiation measured at Schiphol is plotted versus the UHI intensity (Figure 16). In periods where the sun is below or near the horizon ( $Q_{tot} < 100 \text{ W/m}^2$ ), the UHI is positive. During daytime the UHI becomes negative, especially in days with high radiation.

All stations show that the UHI intensity is generally higher at low temperatures (<10 °C), but station #Ams8 (Figure 16, previous page) is the only one with a negative UHI larger than a few tenths of a degree. Station #Ams5 is located adjacent to a large water body and behaves as such (Figure 18), but less clearly than #Ams8 because it is also located near trees and buildings. #Ams10 has a low UHI overall.

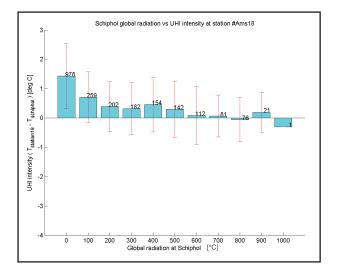


Figure 17: The intensity of the UHI at station #Ams8, depending on the incoming global radiation at reference station Schiphol.

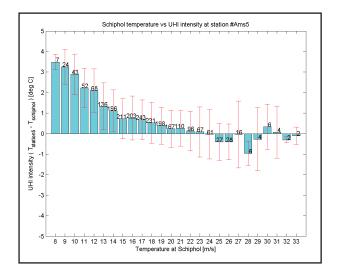


Figure 18: The intensity of the UHI at station #Ams5, depending on the temperature at reference station Schiphol.

All the other stations show the pattern similar to #Ams2 and #Ams12 as depicted in Figures 19 and 120below, but with varying intensities. Interesting is the increase of UHI intensity at very high temperatures (>30 °C) that seems to occur in all stations. The number of observations is low here, because only a few hours with such extreme temperatures were recorded.

Similar plots were made for many different parameters to test our assumptions on the behaviour of the UHI. As expected, the intensity of the Urban Heat Island decreases as wind speed increases as the extra heat in the city is ventilated by the wind. The wind is measured at Schiphol airport at 10

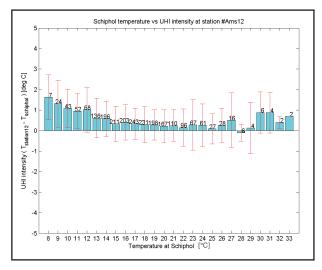


Figure 19: The intensity of the UHI at station #Ams12, depending on the temperature at reference station Schiphol.

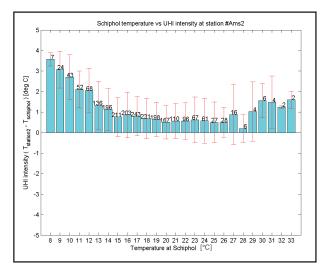


Figure 20: The intensity of the UHI effect at station #Ams2, depending on the temperature at reference station Schiphol.

metres height. For this parameter, all stations show a pattern similar to the one of station #Ams19 and #Ams4 but with varying intensities, as displayed in Figure 21 and 22. In literature, the extinction of wind is expected to follow a logarithmic pattern (*Oke, 1973; Conrads, 1975*) which we also find in these plots. At a first sight, higher wind speeds are recorded at INOORDHO118, the amateur weather station in Amsterdam West. However, this station is located on top of a roof, whereas the wind measurements at Schiphol are at 10 metres height. The wind speeds from Schiphol are extrapolated using the logarithmic wind profile equation to a height of 25 metres, which is the height of the building plus 2 metres for the station pole.

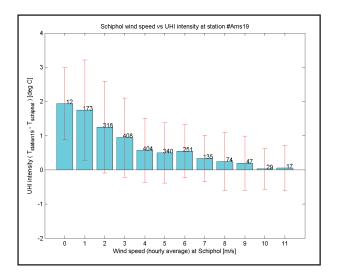


Figure 21: The intensity of the UHI at station #Ams19 depending on the 10m wind speed at reference station Schiphol.

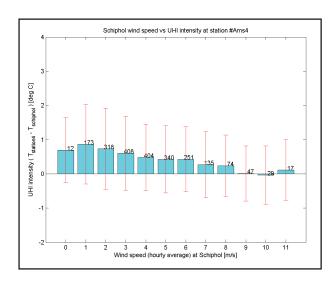


Figure 22: The intensity of the UHI at station #Ams4 depending on the 10m wind speed at reference station Schiphol.

The equation is:

$$U_z = U_{ref} \star ln (z/z_0) / ln (z_{ref}/z_0)$$

where  $U_{ref}$  is the reference wind speed at height  $z_{ref}$  and z is the extrapolation height. For roughness length  $z_0$ , a value of 1.0 m has been chosen which represents "regular large obstacle coverage (suburb, forest)" (*Wieringa, 1986*). Wind roses are plotted in Figure 23 for both stations. The logarithmic extrapolation results in wind speeds that are similar The observation period is June, July and August combined. It is observed that in this period, both stations have dominant wind directions coming from South-West to South-East. The station at Schiphol

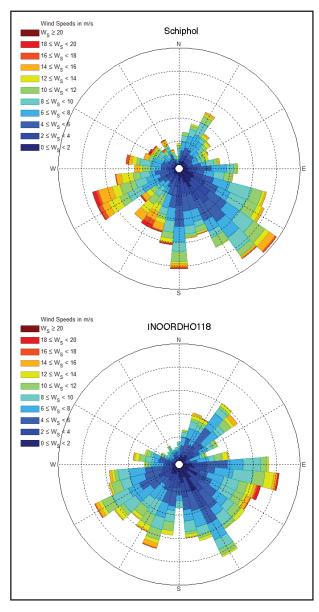


Figure 23: Average wind roses at Schiphol (top) and in Amsterdam (bottom) for June-December 2014.

is assumed to be undisturbed by obstacles, whereas the amateur station is in the middle of the city and could be affected by the morphology of the urban environment. Such a large wind obstruction is found in the southern wind direction.

Other data from the amateur weather station is well in agreement with our own observations at nearby station #Ams13. The average temperature differs only by +0.09 °C and the standard deviation of the difference is 0.33 °C. Relative humidity is underestimated by 2% on average. The pressure measured at Schiphol is 0.1 kPa higher than measured by the amateur weather station. To analyze the UHI intensity on very hot days, a shorter time span was selected. On the 18<sup>th</sup> and 19<sup>th</sup> of July 2014 the Netherlands experienced maximum temperatures above 30 °C in most parts of the country. A high pressure system over Europe resulted in several days with lots of sunshine, no precipitation and low wind speeds. The synoptic weather situation is presented in Figure 25 on the next page.

Schiphol and all weather stations measured the highest temperature during the entire JJA period at either 14:00 UTC or 13:00 UTC on July 19<sup>th</sup>. Only two stations measured a maximum temperature lower than at Schiphol (33.30 °C). At 14:00 UTC, station #Ams8, located on a small island in het IJ #Ams8 records a temperature of 3.2 °C lower than at the reference station. This large difference can be observed in Figure 24 as well and explained by the major availability of water that results in evaporation. Station #Ams5 is located on the built-up Java-island and records 32.9 °C. The presence of a large patch of trees may be the result of a relatively low temperature

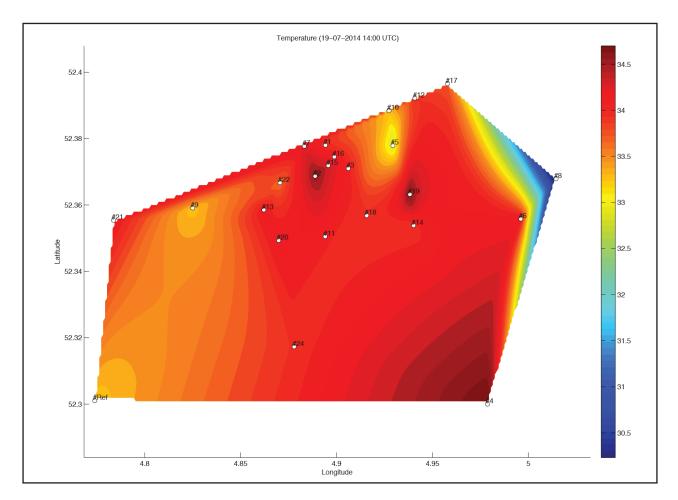


Figure 24: Temperatures measured at the stations (white markers) at 19<sup>th</sup> of July, 14:00 UTC, the warmest recorded hour in the JJA period.

of 33.3 °C at station #Ams10. At #Ams9, a large lake and vegetation is nearby (within 500 m). The highest recorded temperature in the entire period is found in the South-East corner (34.9 °C) at station #Ams4. At this time, differences between the stations and Schiphol are in the range of -3.8 °C and 1.5 °C with an average of 0.6 °C, similar to the overall average UHI effect. However, the largest UHI intensities are not found during midday hours, but in the early evening after a hot day (Figure 26). The concrete, pavement and buildings have absorbed radiation throughout the day and continue to emit this heat for hours. The temperature at the rural area drops as soon as the sun's radiation decreases.

20 out of 23 stations record the highest UHI intensity at 20:00 UTC on either July 18<sup>th</sup> (11 stations) or July 19<sup>th</sup> (9 stations). Stations #Ams8, #Ams10 and #Ams17 are associated with low UHI intensities throughout the period and record their maximum UHI value at 2-7-2014 3:00 UTC, 3-7-2014 23:00 UTC, 4-7-2014 2:00 UTC respectively.

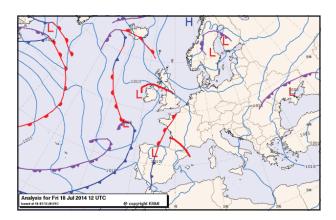


Figure 25: Synoptic weather situation over Europe at the 18th of July 2014, 12:00 UTC. Source: www.knmi.nl

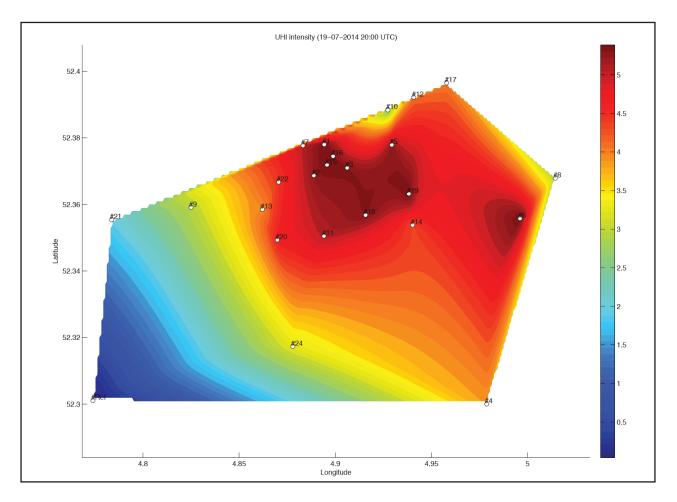


Figure 26: The intensity of the Urban Heat Island at the stations (white markers) at 19<sup>th</sup> of July, 20:00 UTC, one of the hours with the highest UHI intensities in the JJA period.

#### **3.2 WRF MODELLING**

The runtime of WRF depends on the model setup and number of computer processing units that are allocated to the job. Run time for the three WRF runs was in the order of days. The WRF output files are enormous amounts of raw data (in this research over 65 GB!) which makes post-processing necessary. In Table 3, an overview of the different runs is presented with the corresponding names that will be used in the remainder of this report.

Table 3: Overview of the WRF runs in this research.

Run	Name	Details
Run 1	Initial	Initial run
Run 2	Improved	Longer startup, increased SST
Run 3	Perturbed	Temperatures +2 °C

In Figure 27, the temperatures of the fourth domain are given at the warmest hour observed (14:00 UTC at 19<sup>th</sup> of July 2014). It can be observed that the temperature is much lower over water bodies (about 22-25 °C) than over land (about 32-33 °C). There is no clear difference between temperatures within the city and rural areas such as Schiphol (bottom left corner). The difference between water temperatures in the Initial and Improved run is evident: temperatures above water bodies are a few degrees higher in the Improved run. Note that there is a slight shift in the domains orientation in between the runs because of the different domain setup, the dimensions however do not change. Temperatures over land are higher in the Improved run as well. This may be the result of the extra day of start-up time in this run, which lead to higher (and more realistic) soil and building temperatures.

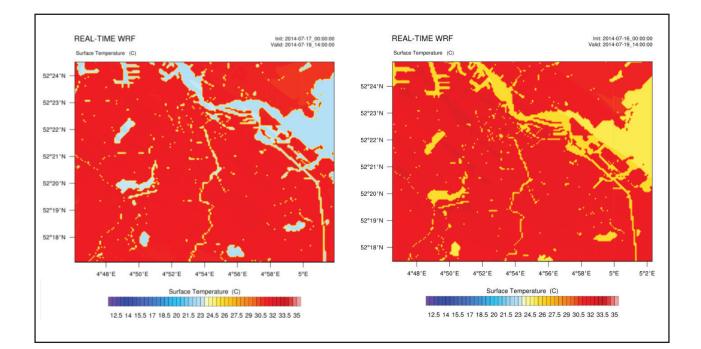


Figure 27: 2 metre temperature of the fourth domain at 19-07-2014 14:00 UTC as modelled by WRF in the Initial run (left) and Improved run (right).

The results of the observations in chapter 3.1 have shown that the largest UHI intensities are found at 20:00 UTC at 18<sup>th</sup> or 19<sup>th</sup> July. The temperatures for these times are presented in Figure 28, which indeed shows a large contrast between the city and its surroundings. The high spatial resolution of this domain results in a very detailed overview of the surface temperature. Individual objects such as rivers or the runways of Schiphol airport are clearly discernible. The difference seems larger at July 19<sup>th</sup> than at the day before that, and smaller in the Improved run than in the Initial run.

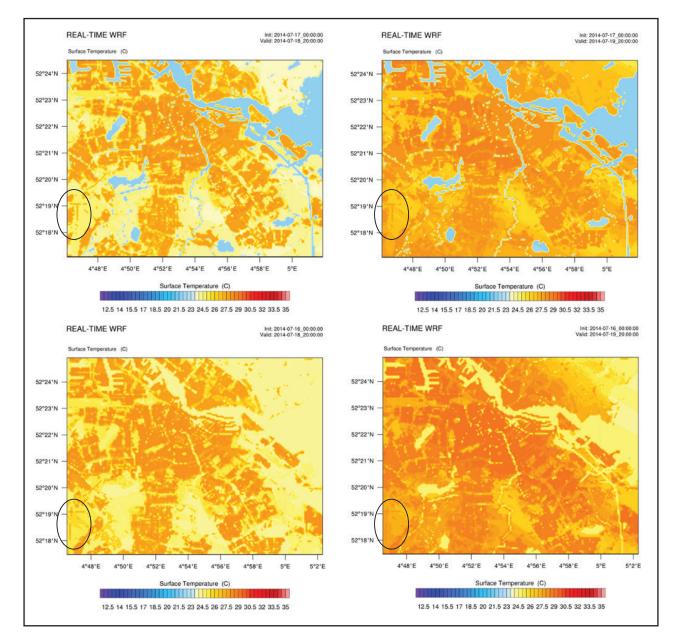


Figure 28: Temperatures for the fourth domain. Top figures show the results of the Initial run at 18-07-2014 20:00 UTC (left) and 19-07-2014 20:00 UTC (right), the bottom row for the Improved run at identical times. The runways of Schiphol airport are encircled.

WRF models differences in temperature between urban and rural areas. This effect is not only visible in the high resolution domain of Amsterdam, but also in larger domains, as can be seen in Figure 29. In this figure, individual cities and even smaller towns can be discerned. The Randstad, a highly urbanized area in the west of the Netherlands, is cluttered with warm areas. The warm places near the coast are most likely the sand dunes that show up because of the high heat capacity of dry sand. Since the water temperatures have been increased in the fourth domain only, they are generally cooler in this figure than in the previous ones. To validate output data from WRF with the actual observations, hourly temperatures are extracted from the WRF model at each grid cell where a weather station is located. In Figure 30, the relation between the modelled and measured temperatures is presented for the two runs. It can be observed that the Initial run models temperatures that are lower than the observations, especially for temperatures below 25 °C. The Improved run performs better here (R<sup>2</sup> from 0.83 to 0.88, RMSE from 2.05 °C to 1.73 °C and Bias from -1.48 °C to -0.99 °C), but the WRF model is still colder than our observations on average. Similar scatter plots were made for each individual station and run, resulting in 46 figures, of which only the most interesting are presented in this report.

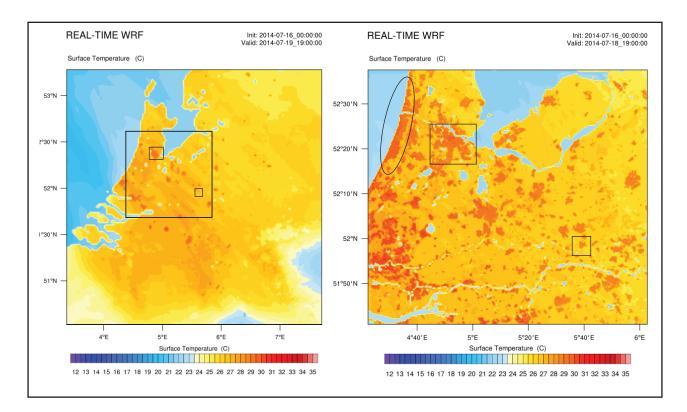


Figure 29: Left: Temperatures in d02 of the Improved run at 18-07-2014 19:00 UTC. Domains d03, d04 and d05 are marked by rectangles. Right: Temperatures in d03 of the Improved run at 19-07-2014 19:00 UTC. Domains d04 and d03 have been marked with a rectangle, warm sand dunes near the coast are encircled.

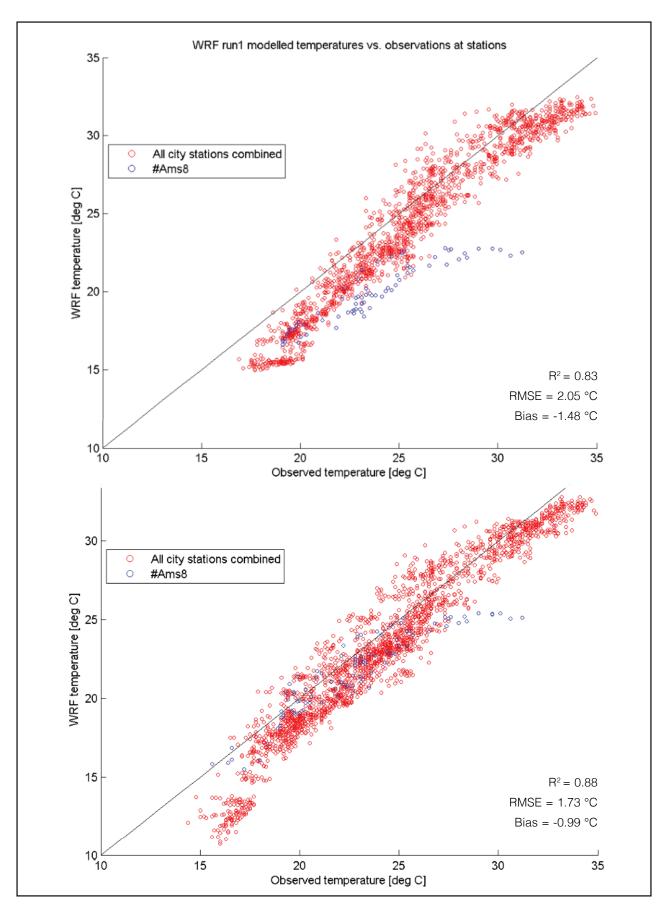


Figure 30: The modelled temperature by WRF in the Initial run (top) and Improved run (bottom) at the stations, versus the observations made at those stations. Blue circles present the temperature relation for water station #Ams8. Total number of circles is 72 hours (top) or 96 hours (bottom) for 23 stations (=1656 or 2208 observations).

The increase of water temperatures and 24 hours more start-up time have increased the accuracy of the WRF model in predicting the urban temperatures. In Figure 31, scatter plots are show for three station for both runs. It can be observed that all trend lines fit better to the 1:1 line in the Improved run. There is no visible decrease of the spread, and temperatures above 30  $^{\circ}$ C are still slightly underestimated by WRF in all cases.

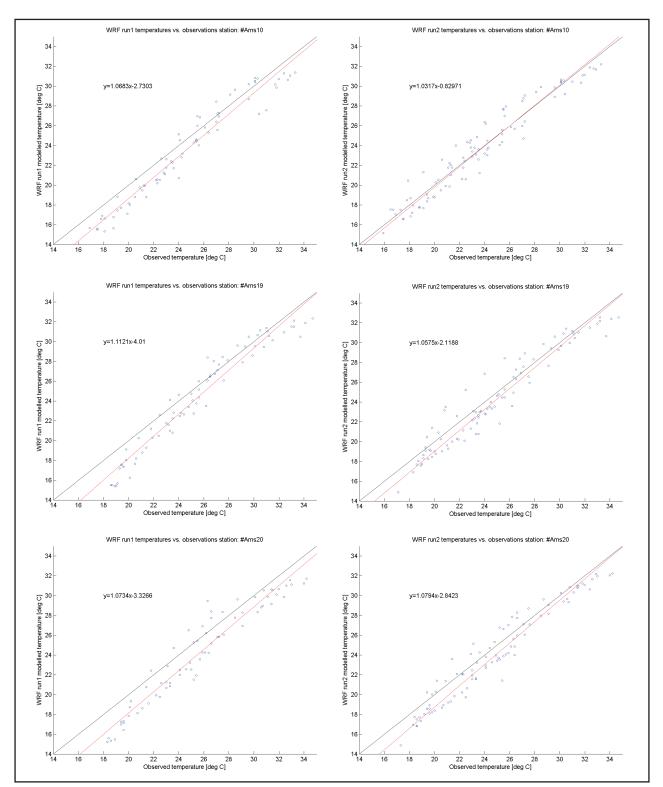


Figure 31: The modelled temperature by WRF versus the observed temperature. Top figures show #Ams10, middle figures #Ams19 and bottom rows is #Ams20. Figures on the left are those for the Initial run, whereas the Improved run can be found on the right side. Red lines are linear trend lines with equations.

#### **3.3 STATISTICAL RELATIONSHIP**

For each of the stations, hourly values of T<sub>urban</sub> were calculated for June, July and August using the statistical relationship from Michiel van der Harst. Table 4 shows the general performance of the calculation. The R<sup>2</sup> and RMSE values for the data from which the formula was derived in Wageningen are 0.97 and 0.89 °C respectively.

Although the relationship is derived for clear, warm days, it performs well over the entire JJA period as well. Only stations #Ams5 and #Ams8 have an  $R^2$ value lower than 0.90, and have the highest RMSE values. A large area of surface water surrounds these two stations whereas all the other stations are typical city stations. Station #Ams24 performs best with an  $R^2$  value of 0.95 and RMSE of 0.94 °C.

If we zoom in on a short, warm period, the performance increases for almost all stations. The performance of water station #Ams5 increases quite a lot, whereas #Ams8 shows a decrease. The other station that appears to perfom less in higher temperatures is #Ams4. This could be associated with the very high temperatures measured at this location. As can be seen in Figure 32, the relationship performs less in extreme temperatures, because in such Table 4: The statistical performance of the statistical relationship derived for Wageningen, applied to the Amsterdam weather stations for two time series.

Station	RMSE	R2	RMSE	R2
	JJA	JJA	11-20	11-20
			July	July
Average	1.16	0.91	1.17	0.92
Ams1	1.18	0.91	1.13	0.92
Ams2	1.21	0.91	1.24	0.91
Ams3	1.23	0.91	1.23	0.91
Ams4	1.10	0.92	1.32	0.90
Ams5	1.41	0.88	1.18	0.92
Ams6	1.14	0.92	1.21	0.91
Ams7	1.21	0.91	1.21	0.91
Ams8	1.65	0.83	1.87	0.80
Ams9	0.95	0.94	0.95	0.95
Ams10	1.13	0.92	1.004	0.94
Ams11	1.19	0.91	1.28	0.90
Ams12	0.97	0.94	0.99	0.94
Ams13	1.21	0.91	1.17	0.92
Ams14	1.20	0.91	1.29	0.90
Ams15	1.24	0.90	1.22	0.91
Ams16	1.15	0.92	1.09	0.93
Ams17	1.03	0.93	0.95	0.95
Ams18	1.17	0.91	1.18	0.92
Ams19	1.17	0.91	1.20	0.91
Ams20	1.10	0.92	1.19	0.92
Ams21	0.87	0.95	0.93	0.95
Ams22	1.16	0.92	1.18	0.92
Ams24	0.90	0.95	0.89	0.95

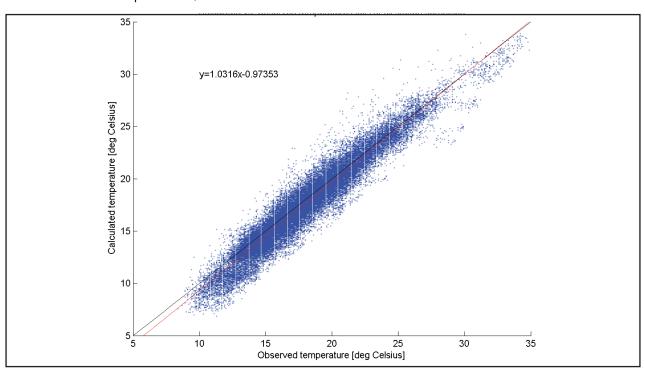


Figure 32: Scatter plot of the calculated urban temperatures versus the actual temperature observations, for all hours in the JJA period and all 23 stations combined.

fundamenatlly different meteorological conditions, other relationships will apply. In the research from Michiel van der Harst, another formula was derived for estimating the daily *maximum* UHI intensity, where for example the fraction of impervious surface was proven to be significant. In the majority of the observations, however, the  $T_{urban}$  equation is useful. For every hour at every station the agreement is plotted above (n=50232, 91 days \* 24 hours \* 23 stations). It can be observed that the more extreme values tend to be underestimated. If the observed temperature is lower than ca. 15 °C or exceeds 30 °C, the relationship underestimates the temperature in most of the cases. These scatter plots have been created for each individual station as well, of which the most interesting are shown in Figure 33. The performance of the statistical

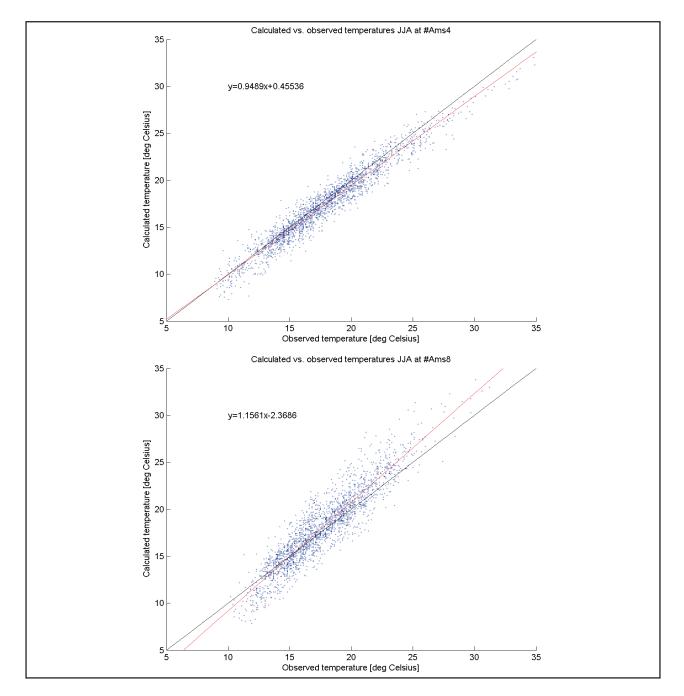


Figure 33: Scatter plot of the calculated urban temperatures versus the actual temperature observations for #Ams4 (top) and #Ams8 (Bottom) for all hours in the JJA period. The red line shows the linear regression between all points.

relation is the lowest at #Ams8, the station located on an island in het IJ. Overestimation of the urban temperature occurs in most of the cases where the observed temperature is T>20 °C. The model has a low performance at station #Ams4 during the warm period. In the corresponding scatter plot it can be observed that the calculation underestimates the actual urban temperature in most of the cases above 25 °C. The linear trend line has a slope lower than 1.0 here, whereas all the other stations have trend lines with slopes between 1.01 and 1.07. Water stations #Ams5 and #Ams8 are high exceptions (1.10 and 1.16 respectively). Here, the relationship substantially underestimates (overestimates) the observed temperature in the coldest (warmest) hours.

In Figure 34, line plots are presented for the calculation and observations of temperature for a few interesting stations. For #Ams24, the relationship performs best in the chosen period. It can be observed that the calculation fits the observations very well with underestimations of up to 2 °C in some nights, which is quite high. During the warmest hours of the day, the calculation can overestimate the temperature in some cases, but predicts the urban temperature accurately in general. As could be expected from the scatter plots, the calculated temperatures are lower than the observations at station #Ams4 in most of the nights and warm hours of the day. The largest underestimation (3.0 °C) during day time occurs when the highest JJA temperature is recorded at this station (34.9 °C at 19-7 13:00 UTC). The calculation shows large overestimations during daytime at station #Ams8. The actual observations are much lower than those in the city, caused by the cooling effect of the water surrounding this station.

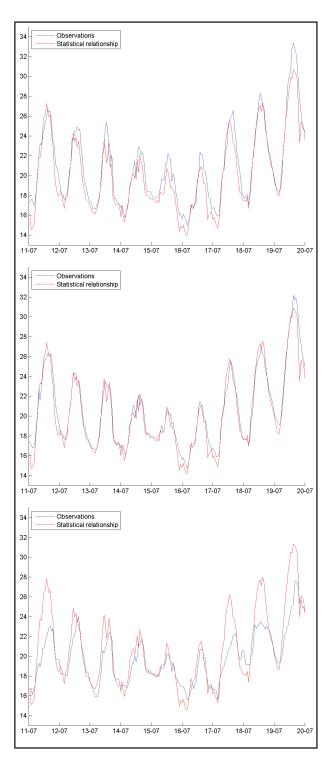


Figure 34: Linear plot of the calculated urban temperatures and the actual temperature observations over time. The relationship performs best at #Ams24 (middle). The largest underestimation of the temperature is visible at #Ams4 (top), whereas the largest overestimation occurs at #Ams8 (bottom).

A first attempt was made to improve the statistical relationship for Amsterdam. The five independent variables that were used in the derivation in Wageningen were included. Additionally, water temperature and water fraction were combined into a an attempt to test if the availability of water has an effect on the Urban Heat Island intensity.

A total of 28152 observations were analysed in a multi-regression analysis. Two out of the six variables were found to be insignificant, the Antecedent Precipitation Index that is used in the Wageningen equation is not significant anymore in Amsterdam, as is the wind speed. The P-values of the other variables are all below 0.001 and thus significant. The equation that is constructed is as follows:

$$T_{urban\_Amsterdam} = 0.9692 * T_{rural} - 0.9654 * NDVI + 6.141e^{-08} * Rad_{urban} + (Frac_{water} * (T_{water} - T_{rural})) + 0.0550$$

And the original equation for Wageningen is:

$$T_{urban_Wageningen} = 0.9765 * T_{rural} - 0.8204 * log (U) - 0.02312 * API - 2.365 * NDVI + 2.392e^{-08} * Rad_{urban} + 2.706$$

This new equation has an R<sup>2</sup>-value of 0.92 and RMSE of 0.91 °C. This is a slightly better performance than using the original Wageningen formula that resulted in values of 0.91 and 1.16 °C respectively. Additional statistics can be found in Table 5. The exclusion of the API is interesting and could be explained by the fact that Amsterdam has more paved surface than Wageningen, which limits the amount of evaporation of soil moisture. The coefficients of the other variables are different, but the effect a variable has on the Urban Heat Island intensity stays constant (either positive or negative). In Amsterdam, the urban temperatures depend more on solar radiation than in Wageningen. NDVI is less effective in decreasing the urban temperature in Amsterdam than it is in Wageningen. Water temperature has a positive (negative) effect on the UHI if it is higher (lower) than the temperature at Schiphol. The fraction of open surface water near the station amplifies this effect.

Table 5: The statistical performance of the improved statistical relationship applied to the Amsterdam weather stations for the two time series also used in Table 4.

Station	RMSE	R2	RMSE	R2
	JJA	JJA	11-20	11-20
			July	July
Average	0.91	0.93	0.97	0.93
Ams1	1.03	0.93	1.09	0.92
Ams2	1.02	0.93	1.15	0.92
Ams3	0.98	0.93	1.09	0.92
Ams4	0.96	0.94	1.11	0.92
Ams5	0.93	0.93	0.98	0.93
Ams6	1.01	0.93	1.08	0.92
Ams7	1.05	0.92	1.13	0.92
Ams8	1.51	0.87	1.44	0.82
Ams9	0.81	0.96	0.84	0.96
Ams10	0.92	0.94	0.83	0.96
Ams11	0.97	0.93	1.15	0.92
Ams12	0.85	0.95	0.84	0.96
Ams13	0.84	0.95	0.92	0.95
Ams14	0.93	0.94	0.98	0.94
Ams15	1.11	0.92	1.17	0.91
Ams16	1.00	0.93	1.06	0.93
Ams17	0.86	0.95	0.83	0.96
Ams18	1.02	0.93	1.09	0.93
Ams19	1.03	0.93	1.08	0.93
Ams20	0.91	0.94	1.01	0.94
Ams21	0.76	0.96	0.84	0.96
Ams22	0.98	0.93	1.09	0.92
Ams24	0.74	0.96	0.76	0.96

# **3.4 FUTURE CLIMATE**

The Perturbed run in WRF had perturbed initial conditions to simulate a warmer climate. All air, water and soil temperatures are increased with 2 °C. In Figure 35, these perturbations are made visible for the initial conditions where the general pattern is the same (but just shifted in colour). The non-linear chaotic nature of meteorology causes temperatures to be different than just a 2 degree perturbation as model time increases. Figure 35 shows the temperatures over Europe under a future

climate during one of the warmest observed hours in Amsterdam in 2014. It is found that some regions in Europe experience extreme temperatures of 35  $^{\circ}$ C and that the North Sea is much warmer.

The modelled temperatures at the weather stations are compared with the observations. The general trend of temperatures in the future climate is that they are higher than the observations and the results of the second WRF run, as would be expected. However, for some hours there are temperature differences of 5 °C as can be seen in Figure 36. Stations #Ams10

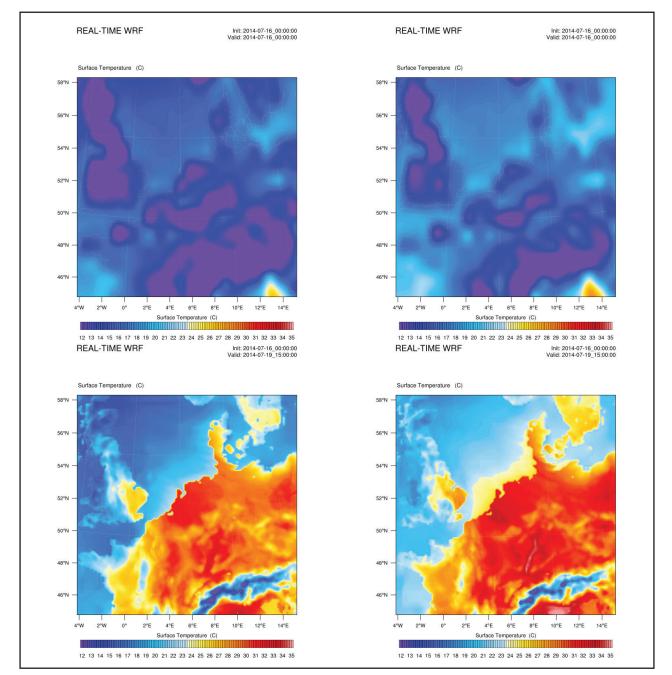


Figure 35: Surface temperatures of domain d01 in the Improved run of WRF (left) and the third WRF run (right). Top figures show the models initial conditions and the bottom figures after 87 hours of model time (19-07-2014 15:00 UTC).

and #Ams20 show such extreme temperatures during daytime. Higher temperatures are especially found at #Ams10 during night time. The station that observed the highest temperatures in 2014 is #Ams4, and these observations are actually higher than the modelled future climate temperatures. It seems that WRF is not capable of modelling the Urban Heat Island effect at this particular location. The temperature evolution at water station #Ams8 is very similar to that of the second WRF run, but shifted up two degrees because the water temperature is not expected to change that rapidly over the course of a few days. It is less 'chaotic' than air temperatures in such a short period. On average, the city will be 24.98 °C, which is 0.87 °C warmer than the observations under the modelled future climate. However, we have to correct for the initial modelling errors of WRF. The output of the second WRF run is used as a reference of the present climate that results in an average city temperature of 23.19 °C. This gives an average urban temperature increase of 1.78 °C in 2050. Stations #Ams10 and #Ams8 will experience an increase of 1.68 °C and 1.96 °C respectively, all other stations fall in that range. This increase is lower than the original perturbation of 2.0 °C. It follows that the increase of the urban temperature will be less than the increase of global climate, likely because the model returns to the energy balance of before the perturbation.

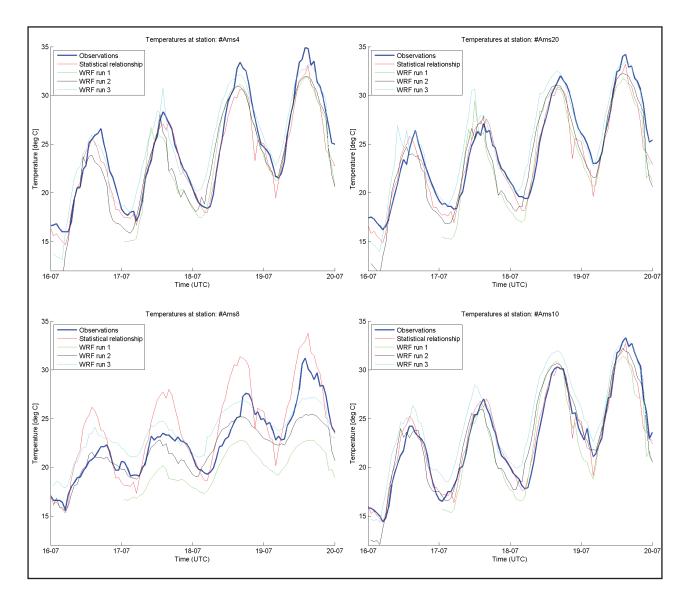


Figure 36: Temperatures at four different stations for 16-20 July 2014. Blue lines show observations, the statistical relationship described in Chapter 3.3 is presented with a red line and the three WRF runs by a green, black and cyan line respectively.

# **4.1 OBSERVATION ANALYSIS**

The initial research questions regarding the observation analysis from the Introduction chapter of this research are:

- Can the installed weather stations be used to find an UHI effect in Amsterdam?

- What is the intensity of this UHI effect and under what meteorological conditions is it the strongest?

- Can we quantify an intra-urban UHI and can this be related to the local urban environment?

The unique setup of the observations in the city has proven to be valuable. The equipment that has been used is identical throughout the city and results in reliable meteorological data in a high time resolution. By comparing the observations to the reference station at Schiphol, an Urban Heat Island effect can be found. Average values for the summer (June, July and August combined) of 2014 range from 0.12 °C to 1.10 °C depending on the station, and 0.67 °C if we combine the temperature at all stations.

On July 18<sup>th</sup> and 19<sup>th</sup> at 20:00 UTC, the highest UHI intensities were measured. At this time, differences in simultaneous temperature observations of 6.1 degrees were recorded between Schiphol and in the city centre (#Ams11, Lutmastraat). The high values were recorded in the evenings (22:00 local time) after hot summer days with maximum temperatures over 30 °C. Meteorological conditions at these days are associated with a high pressure system: low wind speeds and lots of sunshine were able to warm up the city for a few days. The temperatures in the afternoon dropped rapidly at the rural reference when the sun sets, but remain high in the city for the rest of the night (over 3 °C).

There are differences between the UHI intensity within the city. In general, the city centre can be regarded as the thermal core. Most of the stations are located in typical city environments and differences between them can be explained by the availability of trees, water or distance to the centre. Two stations however, are situated near a large water body and temperatures recorded here deviate from those within the city. The water temperature influences air temperature, that sometimes results in negative UHI values for station #Ams8 during night time, with -6.4 °C being the highest negative UHI value found in the JJA period.

It is essential to have reliable measurements at the reference station since they are used to define the intensity of the UHI. However, the choice for a reference station is always a compromise of several factors such as distance to the city, data availability and observation history. It has been shown that measurements at a reference station can be influenced by the ever-expanding city, especially if air is advected by wind over the city before it reaches the reference station. Such effects have been found for Utrecht (*Koopmans et al., 2012*) and Rotterdam (*Heusinkveld et al., 2014*), both cities in the Netherlands.

The measurements at Schiphol could be influenced by the surrounding airport or Amsterdam city nearby as well. To find if such an 'urban induced temperature effect' (UITE) exists, we have averaged the UHI intensity for a few stations depending on the wind direction at Schiphol. Stations #Ams10, #Ams12 and #Ams17 are located in the North East of Amsterdam and close to the edge of the city. Winds coming from this direction are assumed to have 'rural' temperatures. All three stations have a negative UHI intensity if the wind at Schiphol originates from 30 or 40 degrees, with #Ams10 being the most obvious example as can be found in Figure 37. The same figure is created for #Ams20, where we see no such effect but a more circular, 'undisturbed', shape.

This could indicate that Schiphol experiences an urban induced temperature effect as well. If such an effect exists it could mean the results of this research regarding the UHI intensity are underestimated during some conditions. Therefore, another reference station is desired. Since there are no fixed stations in rural areas in the vicinity, a temporary station could

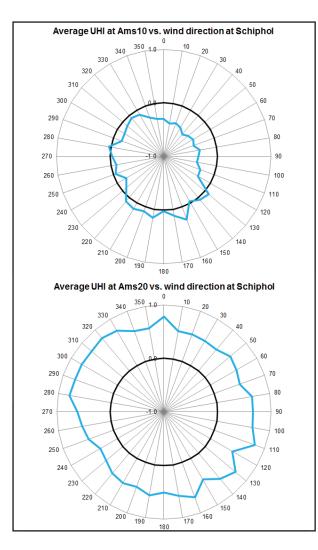


Figure 37: The average intensity of the Urban Heat Island effect for stations #Ams10 (top) and #Ams20 (Bottom), depending on the wind direction at schiphol. The black circle indicates an UHI of 0 degrees. The blue line displays the average Urban Heat Island intensity for each specific direction.

be installed to the North-East of Amsterdam. Here we find many pastures and almost no buildings. This station should be placed well away from the city, but close enough to make realistic comparisons with Schiphol. The indications that urban heat is advected over Schiphol for some wind directions would be an interesting subject for future research.

## 4.2 WRF MODELLING

The original research questions for this part of the research were:

- Can WRF accurately model the temperatures observed at the weather stations?

- (How) can the model be improved to better match the observations?

The output of WRF has been validated using the observations made at the weather stations, but resulted in too low temperatures for most stations after the Initial run. The average bias of this run was -1.51 °C. To improve the skill of the model an additional day of start up time was added. Water temperatures were adjusted to local measurements in the fourth domain instead of using the lower water temperatures from the North Sea that are in the initial NCEP/FNL data. These adaptations resulted in a better performance of the model, with an average bias of -0.98 °C. Station #Ams8 is station that is located on an island which is very complex for WRF to model correctly. The high resolution of the land use maps that are used provide great detail in surface temperatures. These can be very useful to investigate and visualize the intra-urban temperatures. Although temperatures at the weather stations are not always modelled correctly, the outcome of WRF can be used to provide a forecast for temperatures within the city. In extreme temperature cases (temperatures above 30 °C), an underestimation is expected in the forecast. During the night, the city remains warmer than the temperatures modelled in WRF. The daily trend is well captured although actual temperatures from WRF might be off a (few tenths of a) degree Celsius in these extremes. Some of the stations are located near a city canal. Although the resolution of the final domain is high (100 x 100 metres), these water bodies are usually a lot smaller. The grid cell will be regarded as "urban" only and the water effect will be ignored in WRF. Although the weather stations are placed in locations that are as representative as possible, the observations made here are considered as a point measurement, whereas the temperature of WRF is an average over the entire grid cell. It can be expected that comparing such a point measurement with an average temperature over 10000 m<sup>2</sup> gives unreliable results under some conditions.

# **4.3 STATISTICAL RELATIONSHIP**

The initial research questions for this part of the research were:

- Can the statistical relationship that was derived for Wageningen predict urban temperatures in Amsterdam?

- When does the relationship perform best and under what conditions does it fail?

The original statistical relationship performs well in calculating urban temperatures, with R<sup>2</sup> and RMSE values of 0.91 and 1.16 °C respectively in Amsterdam, compared to 0.97 and 0.89 °C in Wageningen (*van der Harst, 2014*). If a smaller, warmer period is selected, the performance increases a little. There are two of the stations that are surrounded by open water where the calculation fails to predict the urban temperature correctly since it was constructed for city stations only. During very high temperatures (>30 °C), it appears that the relationship underestimates the urban temperature.

The temperature during night time hours are underestimated in this period as well, so the relationship works best for temperatures between 15 °C and 25 °C. Temperatures at stations with a large water body nearby are usually overestimated in day time and underestimated during the night, because the original derivation only focused on stations without water. It is fairly easy to use the relationship to come up with an urban temperature. In general, its performance is comparable to that of the WRF model and it requires much less computing time. The disadvantage is that field work has to be performed first (taking sky view photographs) and that it is not as scalable as WRF. The relationship can be used to compare the output of WRF, but will not be able to produce such detailed intra-urban temperatures. An interesting idea is to find a method to approximate the SVF for each grid cell from the land use maps available.

The relationship was derived using observations in Wageningen. Seventeen independent variables were analysed, of which only five were deemed to contribute to the urban temperature. It could be that if a new relationship was constructed for Amsterdam, additional variables (for example the percentage of paved surface near the station) would be considered to be important. In the derivation of the improved relationship for Amsterdam, two additional variables (water fraction and water temperature) were tested and found to improve the relationship.

The availability of satellite images can sometimes be up to one month apart for some locations in Amsterdam. The NDVI values that are derived from these pictures are interpolated for days where no data are available, which could give a simplified version of the NDVI development throughout time. Although only the summer period is considered in this research, there might be unrecorded variations in greenness that would result in different urban temperatures. An extended period of drought could for example decrease the evaporation capabilities of a park in the city.

The original relationship for Wageningen has been improved to match our observations in Amsterdam specifically. Water temperature and surface water fraction have been added to the relationship and the resulting improved equation Amsterdam fits the observation data a little better than the original equation for Wageningen (R<sup>2</sup> shows a minor increase from 0.91 to 0.93, RMSE decreases from 1.16 to 0.91 °C). The effects that radiation (positive) and NDVI (negative) have on the urban temperatures are found in the new equation. The Antecedent Precipitation Index is not significant in Amsterdam in this equation, likely because soil moisture is less available for evaporation in this city. Wind is removed from the equation as well because of its insignificance.

As described in section 4.1, another reference station near Amsterdam would be desired. Stations located in the North of Amsterdam are now located almost 15 km from the reference station, whereas #Ams21 is just 4 kilometres away. Implementing a distance weighted interpolation for these two reference temperatures in the statistical relationship could yield better results. Rather than using the temperature at Schiphol as a reference for calculating the urban temperature, an average depending on the distance to both of the two reference stations could be used.

# **4.4 FUTURE CLIMATE**

The research questions stated in the introduction for this part of the research were:

- Can we predict how the UHI effect will change under a future climate using WRF?

- If so, how large will this change be and what will be the impact on the UHI frequency/intensity.

The final run in WRF started with a temperature perturbation of +2.0 °C. At some stations, the perturbation of initial conditions results in urban temperature differences of almost 5 degrees at certain times. The average increase of urban temperature is 1.78 °C, which is lower than the perturbation. From this WRF experiment, it follows that future urban temperatures will not increase with the same rate as the global temperature increases. However, in this experiment, the only factors that were changed is the temperature increase. Relative

humidity is assumed to stay constant, although this might not be the case for a small period of time. An important factor in Urban Heat Island intensity is the population size (Oke, 1973), which is also kept constant. The land use of the inner city is unlikely to change, but the grasslands surrounding the city might be transformed to urban areas in the coming decades. Implementing these changes of the city in WRF would be an interesting subject of future research. This research could be expanded by investigating which city adaptation measurements are deemed to be most effective in mitigating the Urban Heat Island effect. Several changes in the urban morphology could be tested, such as an increase of surface albedo (more white buildings), increasing the amount of vegetation (planting trees, green roofs) or decreasing the anthropogenic heat flux (reduce energy consumption). By analysing these results, policymakers could implement such adaptation measurements and prevent the detrimental effects on human health of the Urban Heat Island effect.

# **5. LITERATURE**

Brandsma, T., & Wolters, D. (2012). Measurement and statistical modelling of the Urban Heat Island of the city of Utrecht (the Netherlands). Journal of Applied Meteorology and Climatology, 51(6), 1046-1060.

Chen, F., Kusaka, H., Bornstein, R., Ching, J., Grimmond, C. S. B., Grossman, Clarke, S., ... & Zhang, C. (2011). The integrated WRF/urban modelling system: development, evaluation, and applications to urban environmental problems. International Journal of Climatology, 31(2), 273-288.

*Chen, X. L., Zhao, H. M., Li, P. X., & Yin, Z. Y. (2006).* Remote sensing image-based analysis of the relationship between urban heat island and land use/cover changes. Remote sensing of environment, 104(2), 133-146.

*Conrads, L. A. (1975).* Observations of Meteorological Urban Effects: The Heat Island of Utrecht. Rijksuniversiteit te Utrecht

Doherty, R. M., Heal, M. R., Wilkinson, P., Pattenden, S., Vieno, M., Armstrong, B., Stevenson, D. S. (2009). Current and future climate-and air pollution-mediated impacts on human health. Environ Health, 8(suppl 1), S8.

Fallmann, J., Emeis, S., & Suppan, P. (2014). Mitigation of urban heat stress-a modelling case study for the area of Stuttgart. DIE ERDE-Journal of the Geographical Society of Berlin, 144(3-4), 202-216.

- *Gal, T., Lindberg, F., & Unger, J. (2009).* Computing continuous sky view factors using 3D urban raster and vector databases: comparison and application to urban climate. Theoretical and applied climatology, 95(1-2), 111-123.
- *Golden, J. S. (2004).* The built environment induced Urban Heat Island effect in rapidly urbanizing arid regions–a sustainable urban engineering complexity. Environmental Sciences, 1(4), 321-349.

*Touchaei, A. G., & Akbari, H. (2013).* The climate effects of increasing the albedo of roofs in a cold region<sup>†</sup>. Advances in Building Energy Research, 7(2), 186-191.

Harst, Michiel van der – The Urban Heat Island of Wageningen, High spatial resolution measurements and temperature projections in the future, MSc Thesis Wageningen University 2014

Heusinkveld, B. G., Van Hove, L. W. A., Jacobs, C. M. J., Steeneveld, G. J., Elbers, J. A., Moors, E. J., & Holtslag, A. A. M. (2010, April). Use of a mobile platform for assessing urban heat stress in Rotterdam. In Proceedings of the 7th Conference on Biometeorology, Freiburg, Germany (pp. 433-438).

Heusinkveld, B. G., Steeneveld, G. J., Hove, L. W. A., Jacobs, C. M. J., & Holtslag, A. A. M. (2014). Spatial variability of the Rotterdam Urban Heat Island as influenced by urban land use. Journal of Geophysical Research: Atmospheres, 119(2), 677-692.

Hong, S. Y., Noh, Y., & Dudhia, J. (2006). A new vertical diffusion package with an explicit treatment of entrainment processes. Monthly Weather Review, 134(9), 2318-2341.

*Hong, S. Y., & Pan, H. L. (1996).* Nonlocal boundary layer vertical diffusion in a medium-range forecast model. Monthly weather review, 124(10), 2322-2339.

*KNMI (2014),* KNMI'14-klimaatscenario's voor Nederland; Leidraad voor professionals in klimaatadaptatie, KNMI, De Bilt, 34 pp

Koopmans, S., Theeuwes, N. E., Steeneveld, G. J., & Holtslag, A. A. M. (2012). Quantifying the urbanization induced temperature effect of weather station De Bilt (Netherlands) between 1900–2000. In Proceedings of the 8th International Conference on Urban Climates.

*Kusaka, H., Chen, F., Tewari, M., Dudhia, J., Gill, D. O., Duda, M. G., ... & Miya, Y. (2012).* Numerical simulation of Urban Heat Island effect by the WRF Model with 4-km grid increment: an inter-comparison study between the urban canopy model and slab model. Journal of the Meteorological Society of Japan. 90(0), 33-45.

*Lawrence, M. G. (2005).* The relationship between relative humidity and the dewpoint temperature in moist air: A simple conversion and applications. Bulletin of the American Meteorological Society, 86(2), 225-233.

- *Lin, C. Y., Chen, F., Huang, J. C., Chen, W. C., Liou, Y. A., Chen, W. N., & Liu, S. C. (2008).* Urban Heat Island effect and its impact on boundary layer development and land–sea circulation over northern Taiwan. Atmospheric Environment, 42(22), 5635-5649.
- *Luber, G., & McGeehin, M. (2008).* Climate change and extreme heat events. American journal of preventive medicine, 35(5), 429-435.
- Magee, N., Curtis, J., & Wendler, G. (1999). The Urban Heat Island effect at Fairbanks, Alaska. Theoretical and Applied Climatology, 64(1-2), 39-47.
- *Matzarakis, A., Rutz, F., & Mayer, H. (2010).* Modelling radiation fluxes in simple and complex environments: basics of the RayMan model. International Journal of Biometeorology, 54(2), 131-139.
- *Mirzaei, P. A., & Haghighat, F. (2010).* Approaches to study Urban Heat Island–abilities and limitations. Building and Environment, 45(10), 2192-2201.

Morris, C. J. G., Simmonds, I., & Plummer, N. (2001). Quantification of the influences of wind and cloud on the nocturnal Urban Heat Island of a large city. Journal of Applied Meteorology, 40(2), 169-182.

- National Centers for Environmental Prediction/National Weather Service/NOAA/U.S. Department of Commerce, 2000: NCEP FNL Operational Model Global Tropospheric Analyses, continuing from July 1999. Research Data Archive at the National Center for Atmospheric Research, Computational and Information Systems Laboratory, Boulder, CO. [Available online at http://dx.doi.org/10.5065/D6M043C6.] Accessed 14 Dec 2014.
- Oke, T. R. (1973). City size and the Urban Heat Island. Atmospheric Environment (1967), 7(8), 769-779.
- *Population Reference Bureau, (2005):* World Population Data Sheet, Population Reference Bureau 2014, [Available at: http://www.prb.org]
- Robine, J. M., Cheung, S. L. K., Le Roy, S., Van Oyen, H., Griffiths, C., Michel, J. P., & Herrmann, F. R. (2008). Death toll exceeded 70,000 in Europe during the summer of 2003. Comptes rendus biologies, 331(2), 171-178.
- *Ryu, Y. H., Baik, J. J., & Lee, S. H. (2011).* A new single-layer urban canopy model for use in mesoscale atmospheric models. Journal of Applied Meteorology and Climatology, 50(9), 1773-1794.
- Steeneveld, G. J., Koopmans, S., Heusinkveld, B. G., Van Hove, L. W. A., & Holtslag, A. A. M. (2011). Quantifying Urban Heat Island effects and human comfort for cities of variable size and urban morphology in the Netherlands. Journal of Geophysical Research: Atmospheres (1984–2012), 116(D20).
- Steeneveld & G. J., Van Hove, L.W.A. (2010). Een eerste inschatting van het Urban Heat Island effect voor Rotterdam en omgeving een modelstudie. Wageningen University
- Steeneveld, G. J., Koopmans, S., Heusinkveld, B. G., & Theeuwes, N. E. (2014). Refreshing the role of open water surfaces on mitigating the maximum Urban Heat Island effect. Landscape and Urban Planning, 121, 92-96.
- Streutker, D. R. (2003). Satellite-measured growth of the Urban Heat Island of Houston, Texas. Remote Sensing of Environment, 85(3), 282-289.
- *Taha, H. (1997).* Urban climates and heat islands: albedo, evapotranspiration, and anthropogenic heat. Energy and buildings, 25(2), 99-103.
- *Watkins, R., Palmer, J., Kolokotroni, M., & Littlefair, P. (2002).* The London Heat Island: results from summertime monitoring. Building Services Engineering Research and Technology, 23(2), 97-106.
- *Wieringa, J. (1986).* Roughness dependent geographical interpolation of surface wind speed averages. Quarterly Journal of the Royal Meteorological Society, 112(473), 867-889.
- *Willett, K. M., Jones, P. D., Thorne, P. W., & Gillett, N. P. (2010).* A comparison of large scale changes in surface humidity over land in observations and CMIP3 general circulation models. Environmental Research Letters, 5(2), 025210.
- Yang, B., Zhang, Y., & Qian, Y. (2012). Simulation of urban climate with high-resolution WRF model: A case study in Nanjing, China. Asia-Pacific Journal of Atmospheric Sciences, 48(3), 227-241.

# **6. APPENDICES**

# APPENDIX A: DESCRIPTION AND STATISTICS OF WEATHER STATIONS

On the following pages, each of the 24 weather stations is described in terms of environment and observations. A table is presented with an overview of all stations first. Note that the numbering system skips from #Ams22 to #Ams24 since #Ams23 was planned but has never been installed. There are screenshots taken from Google Earth to provide an overview of the surroundings. These screenshots are all facing towards the North and 3D buildings are included if available at that location. The fisheye photographs that were made to determine the sky view factor (as described in chapter 2.1) are transformed into a rectangular coordinate system to provide a 360° panoramic view of the street level.

Name	Latitude	Longitude	Logger	$T_{min}$ (°C)	Time of T <sub>min</sub>	(J <sub>o</sub> ) $_{max}$ ( <sub>O</sub> C)	Time of T <sub>max</sub>	T <sub>avg</sub> (°C)	() (OC) (OC)	UHI <sub>max</sub> (°C)	Time of UHI <sub>max</sub>
Ams1	52,38	4,89	2227	10,40	05/06/2014 04:00	34,00	7/19/2014 13:00	18,29	0,96	5,5	19/07/2014 20:00
Ams2	52,37	4,89	2194	10,20	05/06/2014 04:00	34,60	7/19/2014 14:00	18,25	0,92	5,7	18/07/2014 20:00
Ams3	52,37	4,91	2198	10,10	05/06/2014 05:00	34,10	7/19/2014 14:00	18,18	0,85	5,4	19/07/2014 20:00
Ams4	52,30	4,98	2247	8,90	24/08/2014 04:00	34,90	7/19/2014 13:00	17,85	0,52	4,6	18/07/2014 20:00
Ams5	52,38	4,93	2241	10,00	05/06/2014 05:00	32,90	7/19/2014 14:00	18,06	0,73	5,3	19/07/2014 20:00
Ams6	52,36	5,00	2226	9,80	24/08/2014 04:00	34,20	7/19/2014 14:00	18,07	0,74	5,5	19/07/2014 20:00
Ams7	52,38	4,88	2238	10,30	05/06/2014 04:00	34,30	7/19/2014 14:00	18,34	1,01	5,2	18/07/2014 20:00
Ams8	52,37	5,01	2222	10,20	05/06/2014 07:00	31,20	7/19/2014 13:00	17,57	0,24	4,9	02/07/2014 03:00
Ams9	52,36	4,83	2223	9,70	24/08/2014 03:00	33,70	7/19/2014 13:00	17,73	0,40	5,7	18/07/2014 20:00
Ams10	52,39	4,93	2246	9,10	02/06/2014 04:00	33,30	7/19/2014 14:00	17,45	0,12	4,5	03/07/2014 23:00
Ams11	52,35	4,89	2236	10,00	05/06/2014 04:00	34,10	7/19/2014 14:00	18,20	0,87	6,1	18/07/2014 20:00
Ams12	52,39	4,94	2228	8,70	23/08/2014 05:00	34,00	7/19/2014 14:00	17,74	0,41	4,2	19/07/2014 20:00
Ams13	52,36	4,86	2230	9,60	24/08/2014 03:00	34,20	7/19/2014 14:00	17,99	0,66	5,9	18/07/2014 20:00
Ams14	52,35	4,94	2221	9,10	24/08/2014 04:00	34,00	7/19/2014 14:00	17,71	0,38	4,8	18/07/2014 20:00
Ams15	52,37	4,90	2229	10,40	05/06/2014 04:00	34,40	7/19/2014 14:00	18,43	1,10	5,5	19/07/2014 20:00
Ams16	52,37	4,90	2245	10,30	05/06/2014 04:00	34,20	7/19/2014 14:00	18,35	1,02	5,4	19/07/2014 20:00
Ams17	52,40	4,96	2195	9,50	02/06/2014 04:00	33,80	7/19/2014 14:00	17,73	0,39	4,4	04/07/2014 02:00
Ams18	52,36	4,92	2235	9,90	05/06/2014 04:00	34,00	7/19/2014 14:00	18,17	0,84	5,4	19/07/2014 20:00
Ams19	52,36	4,94	2231	9,80	05/06/2014 04:00	34,70	7/19/2014 14:00	18,11	0,78	5,5	19/07/2014 20:00
Ams20	52,35	4,87	2237	9,90	05/06/2014 04:00	34,20	7/19/2014 14:00	18,04	0,71	6,0	18/07/2014 20:00
Ams21	52,36	4,78	2239	9,70	21/08/2014 05:00	34,30	7/19/2014 13:00	17,75	0,42	6,2	18/07/2014 20:00
Ams22	52,37	4,87	2225	10,20	05/06/2014 04:00	33,70	7/19/2014 14:00	18,20	0,87	6,1	18/07/2014 20:00
Ams24	52,32	4,88	2199	8,40	06/06/2014 04:00	34,20	7/19/2014 13:00	17,76	0,43	5,1	18/07/2014 20:00
Ams25			2240								

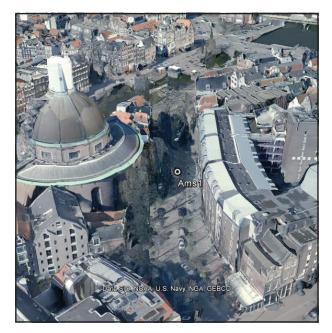
		Time of LIII	A	A . 12	A	A. in a second second second	1 1 / - + E + + +	Current function	0	A d duces
			NDVI (-)	Aveluge RH (%)	Averuge T <sub>dewpoint</sub> (°C)	Averuge pussiule sun hours	700 m (-)	ысыл) испол 300 m (-)	sky view Factor	Audress
Ams1 -	-2,5	7/28/2014 13:00	0,21	69,84	12,46	3,7	0,09	0,00	0,30	Kattengat
Ams2 -	-2,3	7/26/2014 13:00	0,26	60'09	12,27	8,2	0,08	0,00	0,52	Spuiplein
Ams3 -	-2,6	7/28/2014 13:00	0,26	66,77	11,70	4,0	0,23	0,00	0,29	Nieuwe Uilenburgerstraat
Ams4 -:	-3,6	8/20/2014 6:00	0,40	76,42	13,34	8,9	0,03	0,36	0,58	Streefkerstraat
Ams5	-3,1	8/5/2014 15:00	0,41	73,49	13,06	11,9	0,62	0,03	0,63	Javakade
Ams6	-3,8	6/9/2014 16:00	0,19	75,80	13,47	9,1	0,16	0,01	0,57	IJburglaan
Ams7 -	-2,4	8/11/2014 12:00	0,23	69,46	12,45	3,2	0,04	0,01	0,19	Anjelierstraat
Ams8   -(	-6,4	6/7/2014 16:00	0,16	72,40	12,42	15,5	1,00	0,00	1,00	Natuureiland IJburg
Ams9	-3,6	8/11/2014 12:00	0,37	72,84	12,57	7,8	0,00	0,12	0,47	Comeniusstraat
Ams10	-5,7	8/5/2014 16:00	0,54	70,58	11,82	10,4	0,00	0,26	0,43	Zamenhofstraat
Ams11 -	-2,6	8/18/2014 12:00	0,32	71,72	12,76	5,5	0,08	0,00	0,34	Lutmastraat
Ams12	-3,9	8/5/2014 15:00	0,37	71,28	12,25	13,4	0,08	0,32	0,75	Purmerweg
Ams13 -	-2,8	8/11/2014 12:00	0,48	71,59	12,55	4,7	0,08	0,27	0,41	Saxenburgerdwarsstraat
Ams14	-3,5	8/5/2014 16:00	0,54	73,63	12,71	4,9	0,00	0,05	0,28	Galileiplantsoen
Ams15 -	-2,4	6/9/2014 13:00	0,16	68,88	12,42	10,7	0,03	0,00	0,62	Oudezijdsvoorburgwal
Ams16 -	-2,2	8/11/2014 12:00	0,10	69,24	12,44	8,4	0,13	0,00	0,51	Oudezijdsvoorburgwal
Ams17	-3,5	8/5/2014 15:00	0,39	77,59	13,52	10,3	0,00	0,25	0,66	Markengauw
Ams18 -	-2,9	8/23/2014 9:00	0,24	68,61	12,08	8,2	0,00	0,12	0,35	Tweede Oosterparkstraat
Ams19 -	-2,7	8/23/2014 9:00	0,28	70,53	12,46	6,9	0,00	0,00	0,35	Benkoelenstraat
Ams20 -	-2,6	8/18/2014 12:00	0,35	69,89	12,24	4,9	0,00	0,00	0,35	Raephaelstraat
Ams21 -	-2,5	8/18/2014 11:00	0,30	69,03	11,77	11,6	0,00	0,04	0,73	Kwelderweg
Ams22 -	-2,3	8/11/2014 12:00	0,24	72,34	12,90	10,6	0,08	0,00	0,64	Kinkerstraat
Ams24	-3,0	8/17/2014 22:00	0,39	71,57	12,29	13,6	0,00	0,17	0,75	Saskia van Uylenburgweg
Ams25						2,3			0,30	Gustav Mahlerplein

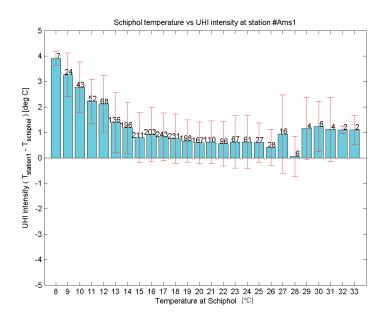


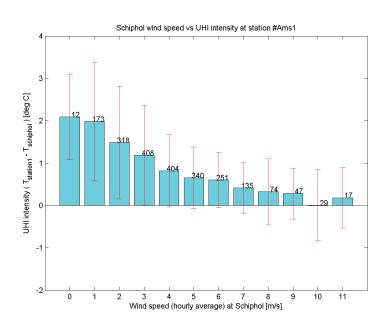
Logger number Latitude Longitude Elevation ASL Sky-view-factor Average NDVI Building presence Building height Vegetation Water Traffic People 2227 N 52.3780 E 4.8942 1.0 m 0.304 0.213 Surrounded by buildings Very high (>20m) A few trees Small water body nearby Some Some June, July, August:

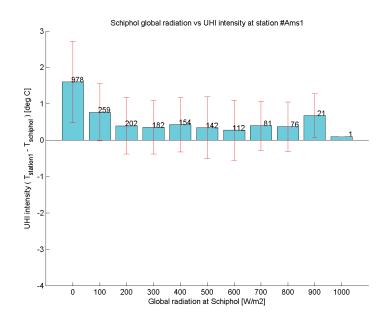
18.29 °C Average temperature Average UHI 0.96 °C Average RH 69.84 % Average dew point temp 12.46 °C Maximum temperature 34.00 °C Recorded at: 19-7-2014 13:00 Minimum temperature 10.40 °C Recorded at: 05-06-2014 04:00 Max UHI 5.5 °C Recorded at: 19-07-2014 20:00 -2.5 °C Min UHI Recorded at: 28-7-2014 13:00 Average unobstructed solar possible using SVF photos: 3.7 hours / day











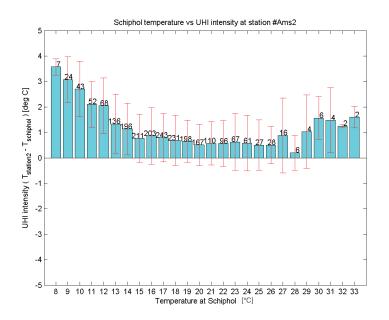


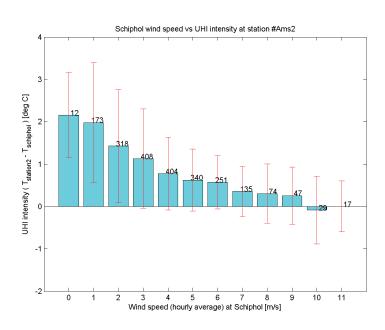
Logger number Latitude Longitude Elevation ASL Sky-view-factor Average NDVI Building presence Building height Vegetation Water Traffic People 2194 N 52.3687 E 4.8888 3.0 m 0.516 0.258 Surrounded by buildings High (15-20m) Trees every few metres Small water body nearby Busy Very crowded June, July, August:

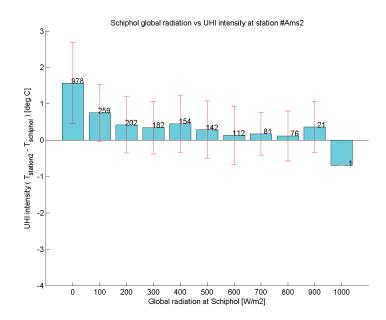
18.25 °C Average temperature Average UHI 0.92 °C Average RH 69.09 % Average dew point temp 12.27 °C Maximum temperature 34.60 °C Recorded at: 19-7-2014 14:00 Minimum temperature 10.20 °C Recorded at: 05-06-2014 04:00 Max UHI 5.7 °C Recorded at: 18-07-2014 20:00 -2.3 °C Min UHI Recorded at: 26-7-2014 13:00 Average unobstructed solar possible using SVF photos: 8.2 hours / day











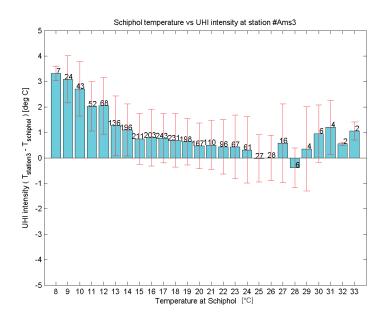


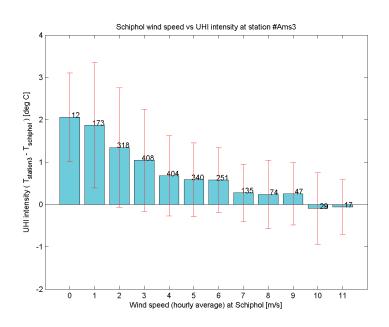
Logger number Latitude Longitude Elevation ASL Sky-view-factor Average NDVI Building presence Building height Vegetation Water Traffic People 2198 N 52.3710 E 4.9062 2.0 m 0.287 0.255 Surrounded by buildings High (15-20m) Trees every few metres Small water body nearby Some Some June, July, August:

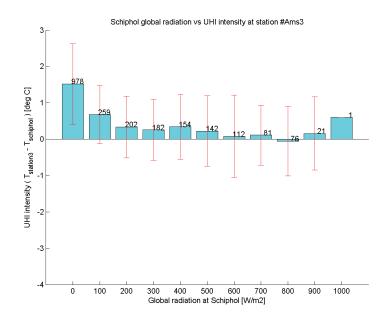
18.18 °C Average temperature Average UHI 0.85 °C Average RH 66.77 % Average dew point temp 11.70 °C Maximum temperature 34.10 °C Recorded at: 19-7-2014 14:00 Minimum temperature 10.10 °C Recorded at: 05-06-2014 05:00 Max UHI 5.4 °C Recorded at: 19-07-2014 20:00 -2.6 °C Min UHI Recorded at: 28-7-2014 13:00 Average unobstructed solar possible using SVF photos: 4.0 hours / day











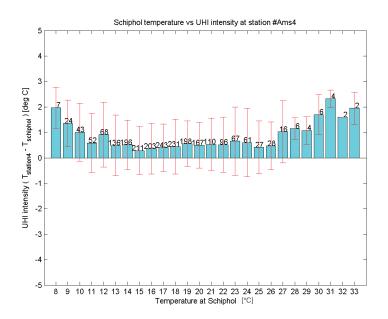


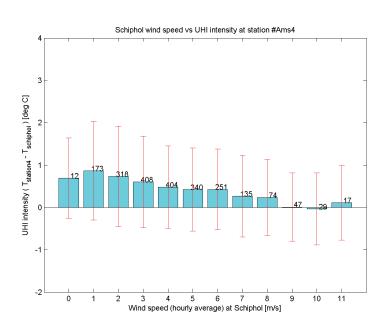
Logger number Latitude Longitude Elevation ASL Sky-view-factor Average NDVI Building presence Building height Vegetation Water Traffic People 2247 N 52.3000 E 4.9787 3.0 m 0.576 0.399 Surrounded by buildings Normal (10-15m) Trees every few metres No Some Some June, July, August:

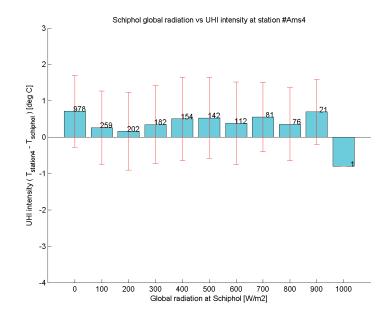
17.85 °C Average temperature Average UHI 0.52 °C Average RH 76.42 % Average dew point temp 13.34 °C Maximum temperature 34.90 °C Recorded at: 19-7-2014 13:00 Minimum temperature 8.90 °C Recorded at: 24-08-2014 04:00 Max UHI 4.6 °C Recorded at: 18-07-2014 20:00 -3.6 °C Min UHI Recorded at: 20-8-2014 6:00 Average unobstructed solar possible using SVF photos: 8.9 hours / day











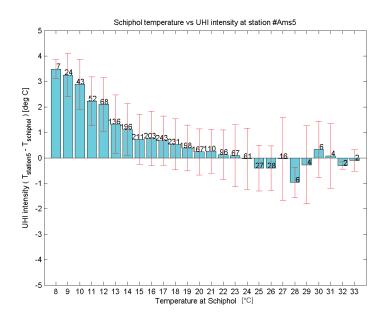


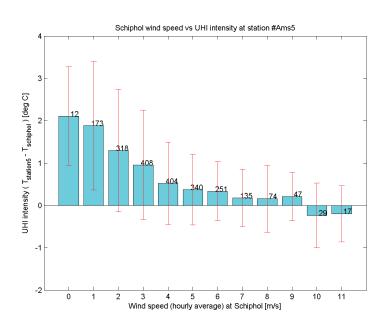
Logger number Latitude Longitude Elevation ASL Sky-view-factor Average NDVI Building presence Building height Vegetation Water Traffic People 2241 N 52.3779 E 4.9294 O.0 m O.632 O.405 Partly built Very high (>20m) No Surrounded by open water No Some June, July, August:

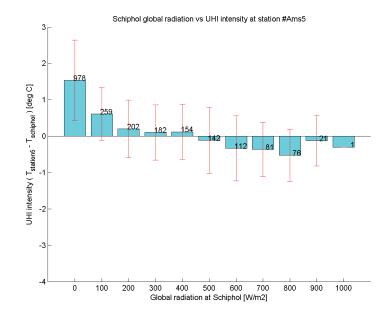
18.06 °C Average temperature Average UHI 0.73 °C Average RH 73.49 % Average dew point temp 13.06 °C Maximum temperature 32.90 °C Recorded at: 19-7-2014 14:00 Minimum temperature 10.00 °C Recorded at: 05-06-2014 05:00 Max UHI 5.3 °C Recorded at: 19-07-2014 20:00 -3.1 °C Min UHI Recorded at: 5-8-2014 15:00 Average unobstructed solar possible using SVF photos: 11.9 hours / day









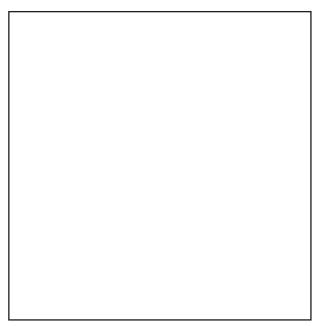


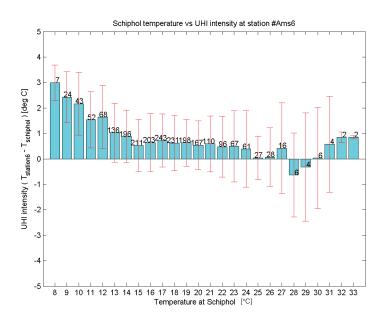


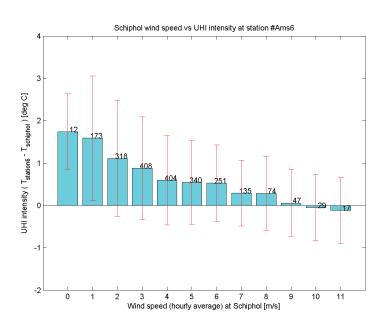
Logger number Latitude Longitude Elevation ASL Sky-view-factor Average NDVI Building presence Building height Vegetation Water Traffic People 2226 N 52.3558 E 4.9960 3.0 m 0.566 0.192 Surrounded by buildings High (15-20m) A few trees Large water body nearby Some Some June, July, August:

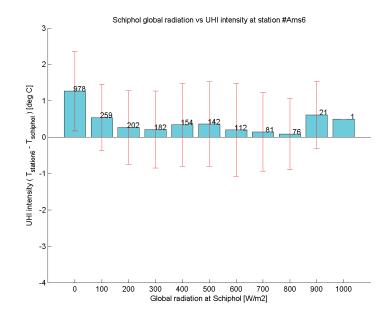
18.07 °C Average temperature Average UHI 0.74 °C Average RH 75.80 % Average dew point temp 13.47 °C Maximum temperature 34.20 °C Recorded at: 19-7-2014 14:00 Minimum temperature 9.80 °C Recorded at: 24-08-2014 04:00 Max UHI 5.5 °C Recorded at: 19-07-2014 20:00 -3.8 °C Min UHI Recorded at: 9-6-2014 16:00 Average unobstructed solar possible using SVF photos: 9.1 hours / day











# #Ams7 - Anjelierstraat

## Metadata:

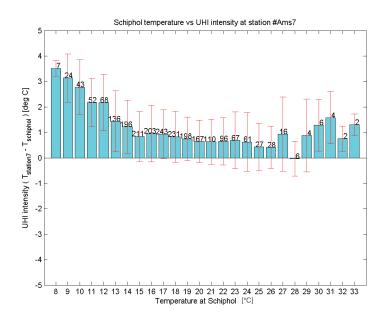
- Logger number Latitude Longitude Elevation ASL Sky-view-factor Average NDVI Building presence Building height Vegetation Water Traffic People
- 2238 N 52.3777 E 4.8832 1.0 m 0.186 0.228 Surrounded by buildings High (15-20m) No No Some Some Some

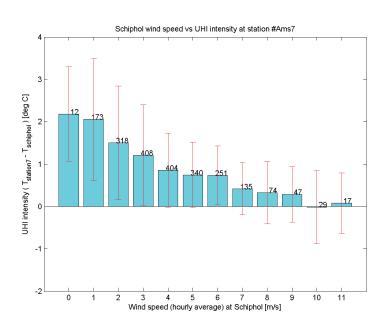
# June, July, August:

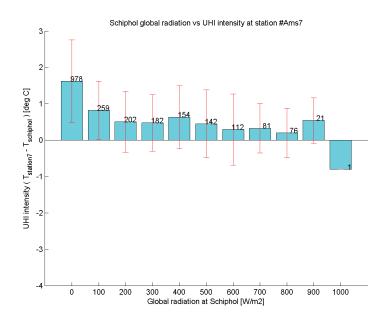
18.34 °C Average temperature Average UHI 1.01 °C Average RH 69.46 % Average dew point temp 12.45 °C Maximum temperature 34.30 °C Recorded at: 19-7-2014 14:00 Minimum temperature 10.30 °C Recorded at: 05-06-2014 04:00 Max UHI 5.2 °C Recorded at: 18-07-2014 20:00 -2.4 °C Min UHI Recorded at: 11-8-2014 12:00 Average unobstructed solar possible using SVF photos: 3.2 hours / day

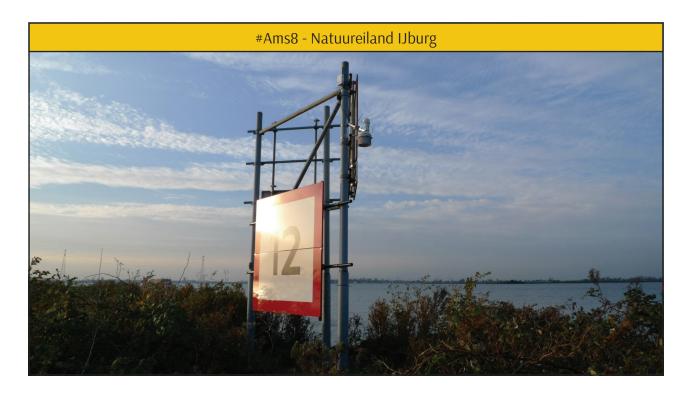












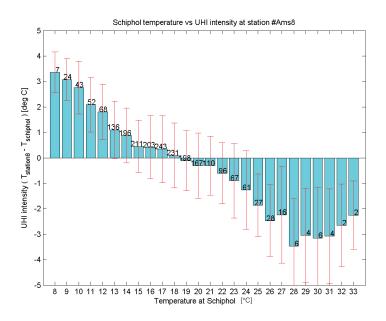
- Logger number Latitude Longitude Elevation ASL Sky-view-factor Average NDVI Building presence Building height Vegetation Water Traffic People
- 2222 N 52.3679 E 5.0144 O.0 m 1.000 O.164 No buildings -No Surrounded by open water No No

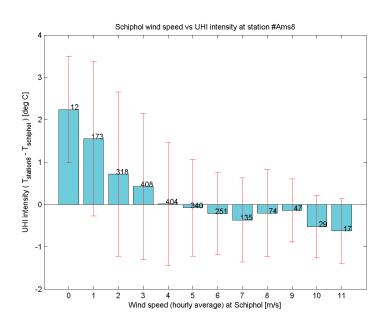
# June, July, August:

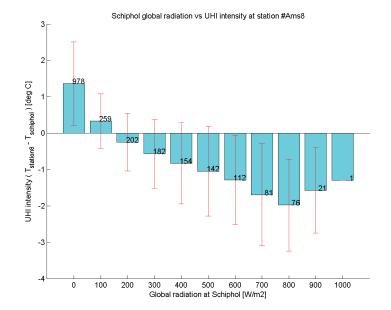
Average temperature	17.57 °C
Average UHI	0.24 °C
Average RH	72.40 %
Average dew point temp	12.42 °C
Maximum temperature	31.20 °C
Recorded at:	19-7-2014 13:00
Minimum temperature	10.20 °C
Recorded at:	05-06-2014 07:00
Max UHI	4.9 °C
Recorded at:	02-07-2014 03:00
Min UHI	-6.4 °C
Recorded at:	7-6-2014 16:00
Average unobstructed solar	
possible using SVF photos:	15.5 hours / day

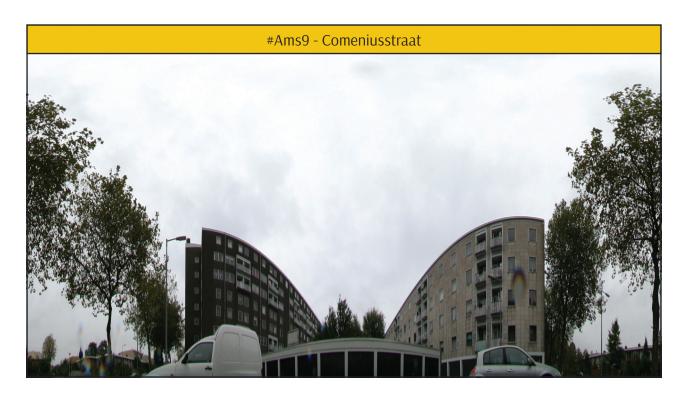












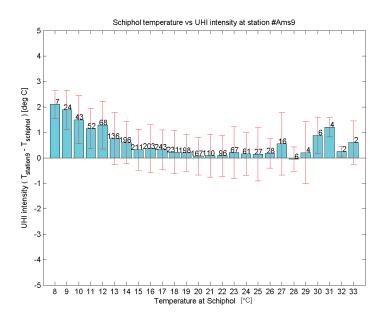
- Logger number Latitude Longitude Elevation ASL Sky-view-factor Average NDVI Building presence Building height Vegetation Water Traffic People
- 2223 N 52.3591 E 4.8250 0.0 m 0.466 0.368 Surrounded by buildings Normal (10-15m) A few trees No Some No

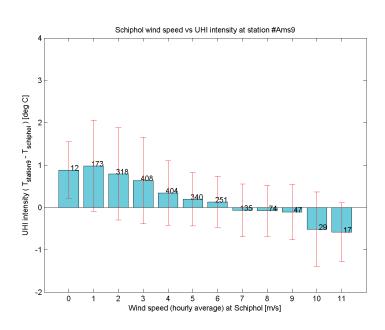
# June, July, August:

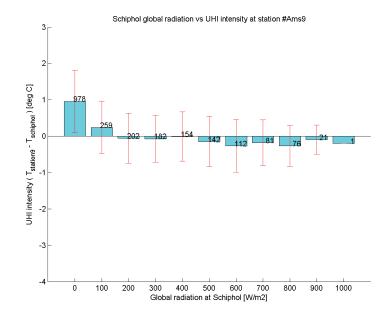
17.73 °C Average temperature Average UHI 0.40 °C Average RH 72.84 % Average dew point temp 12.57 °C Maximum temperature 33.70 °C Recorded at: 19-7-2014 13:00 Minimum temperature 9.70 °C Recorded at: 24-08-2014 03:00 Max UHI 5.7 °C Recorded at: 18-07-2014 20:00 -3.6 °C Min UHI Recorded at: 11-8-2014 12:00 Average unobstructed solar possible using SVF photos: 7.8 hours / day













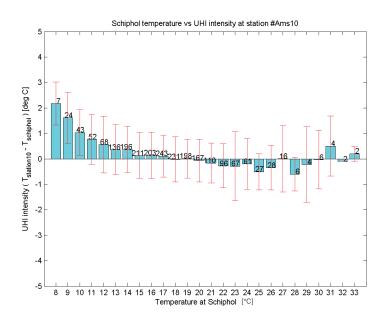
Logger number Latitude Longitude Elevation ASL Sky-view-factor Average NDVI Building presence Building height Vegetation Water Traffic People 2246 N 52.3884 E 4.9274 1.0 m 0.426 0.539 Partly built Normal (10-15m) Many trees nearby No Some No

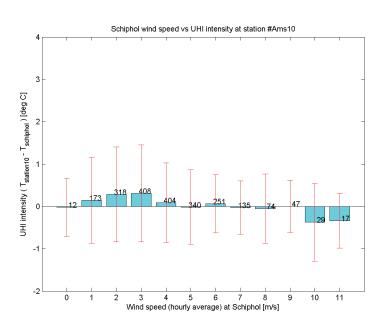
# June, July, August:

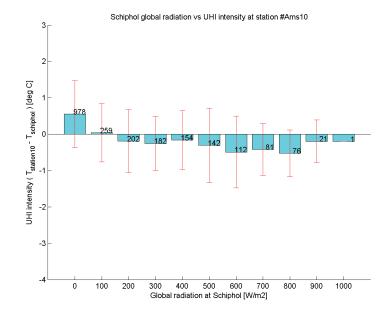
17.45 °C Average temperature Average UHI 0.12 °C Average RH 70.58 % Average dew point temp 11.82 °C Maximum temperature 33.30 °C Recorded at: 19-7-2014 14:00 Minimum temperature 9.10 °C Recorded at: 02-06-2014 04:00 Max UHI 4.5 °C Recorded at: 03-07-2014 23:00 -5.7 °C Min UHI Recorded at: 5-8-2014 16:00 Average unobstructed solar possible using SVF photos: 10.4 hours / day











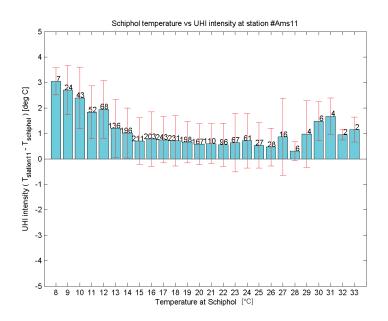


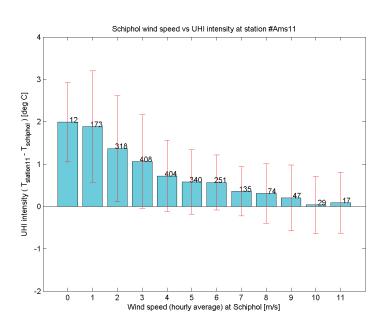
Logger number Latitude Longitude Elevation ASL Sky-view-factor Average NDVI Building presence Building height Vegetation Water Traffic People 2236 N 52.3505 E 4.8941 3.0 m 0.335 0.317 Surrounded by buildings Normal (10-15m) A few trees No Some Some June, July, August:

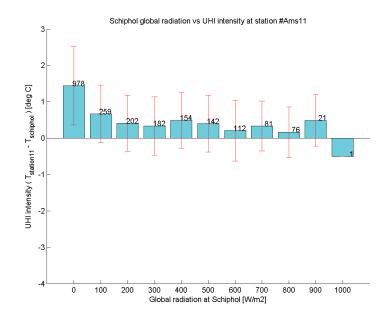
18.20 °C Average temperature Average UHI 0.87 °C Average RH 71.72 % Average dew point temp 12.76 °C Maximum temperature 34.10 °C Recorded at: 19-7-2014 14:00 Minimum temperature 10.00 °C Recorded at: 05-06-2014 04:00 Max UHI 6.1 °C Recorded at: 18-07-2014 20:00 -2.6 °C Min UHI Recorded at: 18-8-2014 12:00 Average unobstructed solar possible using SVF photos: 5.5 hours / day













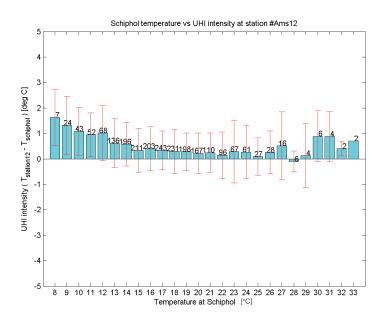
Logger number Latitude Longitude Elevation ASL Sky-view-factor Average NDVI Building presence Building height Vegetation Water Traffic People 2228 N 52.3922 E 4.9408 1.0 m 0.753 0.365 Partly built Normal (10-15m) Trees every few metres No Normal Some

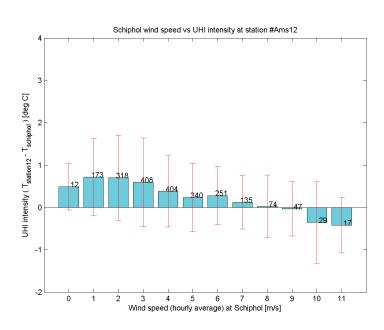
# June, July, August:

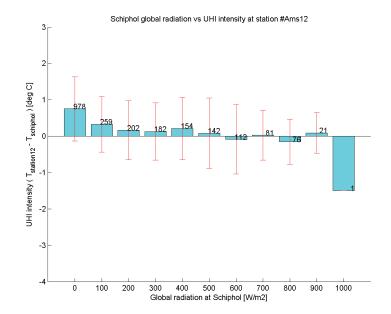
Average temperature	17.74 °C
Average UHI	0.41 °C
Average RH	71.28 %
Average dew point temp	12.25 °C
Maximum temperature	34.00 °C
Recorded at:	19-7-2014 14:00
Minimum temperature	8.70 °C
Recorded at:	23-08-2014 05:00
Max UHI	4.2 °C
Recorded at:	19-07-2014 20:00
Min UHI	-3.9 °C
Recorded at:	5-8-2014 15:00
Average unobstructed solar	
possible using SVF photos:	13.4 hours / day













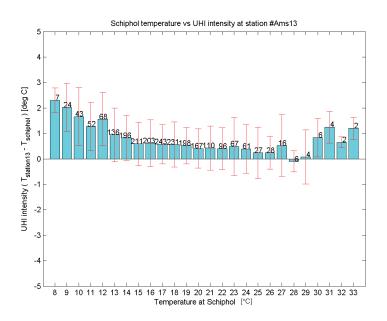
- Logger number Latitude Longitude Elevation ASL Sky-view-factor Average NDVI Building presence Building height Vegetation Water Traffic People
- 2230 N 52.3585 E 4.8621 0.0 m 0.407 0.484 Surrounded by buildings High (15-20m) No No Some Some Some

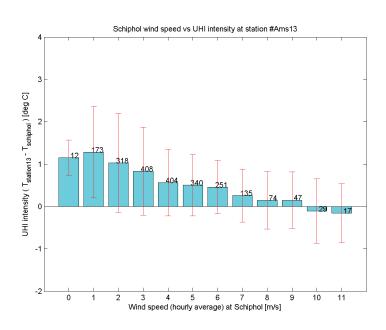
# June, July, August:

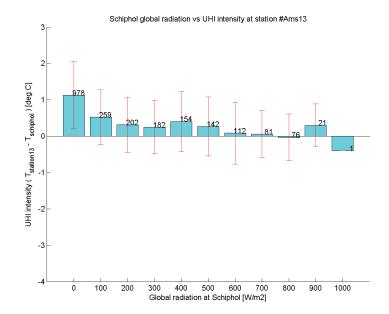
17.99 °C Average temperature Average UHI 0.66 °C Average RH 71.59 % Average dew point temp 12.55 °C Maximum temperature 34.20 °C Recorded at: 19-7-2014 14:00 Minimum temperature 9.60 °C Recorded at: 24-08-2014 03:00 Max UHI 5.9 °C Recorded at: 18-07-2014 20:00 -2.8 °C Min UHI Recorded at: 11-8-2014 12:00 Average unobstructed solar possible using SVF photos: 4.7 hours / day











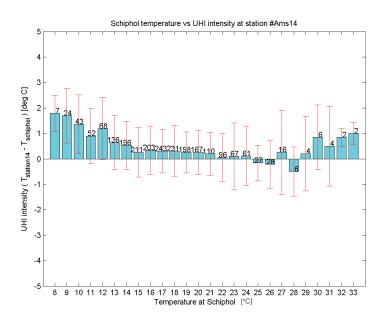


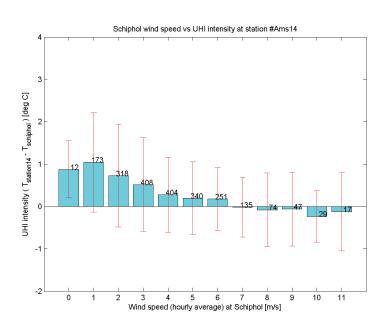
Logger number Latitude Longitude Elevation ASL Sky-view-factor Average NDVI Building presence Building height Vegetation Water Traffic People 2221 N 52.3538 E 4.9402 -2.0 m 0.282 0.542 Surrounded by buildings Normal (10-15m) A few trees Small water body nearby Normal Normal June, July, August:

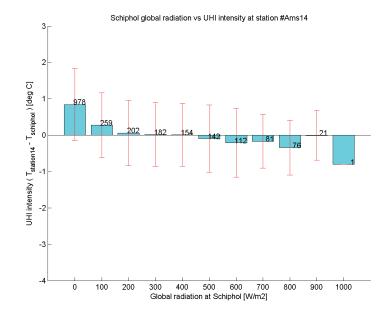
Average temperature	17.71 °C
Average UHI	0.38 °C
Average RH	73.63 %
Average dew point temp	12.71 °C
Maximum temperature	34.00 °C
Recorded at:	19-7-2014 14:00
Minimum temperature	9.10 °C
Recorded at:	24-08-2014 04:00
Max UHI	4.8 °C
Recorded at:	18-07-2014 20:00
Min UHI	-3.5 °C
Recorded at:	5-8-2014 16:00
Average unobstructed solar	
possible using SVF photos:	4.9 hours / day











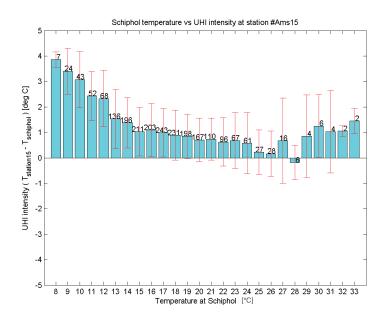


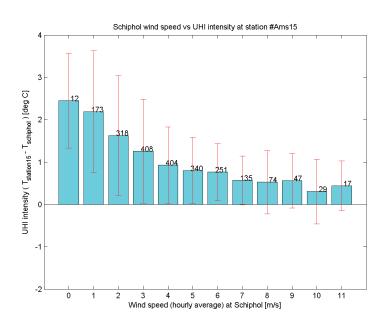
Logger number Latitude Longitude Elevation ASL Sky-view-factor Average NDVI Building presence Building height Vegetation Water Traffic People 2229 N 52.3719 E 4.8957 1.0 m 0.621 0.159 Surrounded by buildings High (15-20m) A few trees Small water body nearby Busy Very crowded June, July, August:

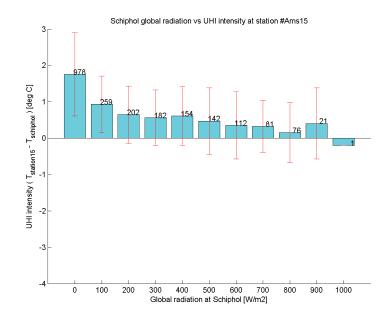
18.43 °C Average temperature Average UHI 1.10 °C Average RH 68.88 % Average dew point temp 12.42 °C Maximum temperature 34.40 °C Recorded at: 19-7-2014 14:00 Minimum temperature 10.40 °C Recorded at: 05-06-2014 04:00 Max UHI 5.5 °C Recorded at: 19-07-2014 20:00 -2.4 °C Min UHI Recorded at: 9-6-2014 13:00 Average unobstructed solar possible using SVF photos: 10.7 hours / day











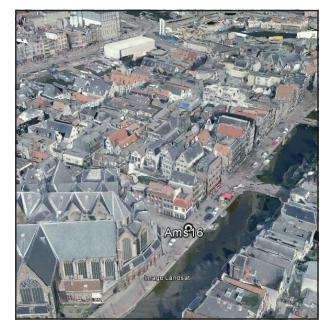


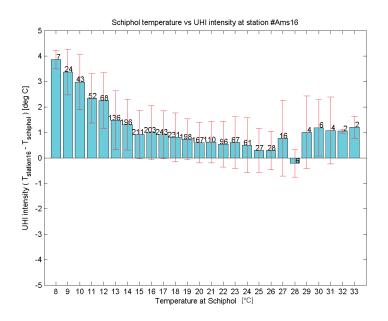


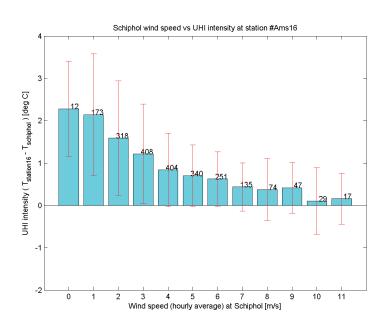
Logger number Latitude Longitude Elevation ASL Sky-view-factor Average NDVI Building presence Building height Vegetation Water Traffic People 2245 N 52.3745 E 4.8989 1.0 m 0.513 0.102 Surrounded by buildings Very high (>20m) A few trees Small water body nearby Busy Very crowded June, July, August:

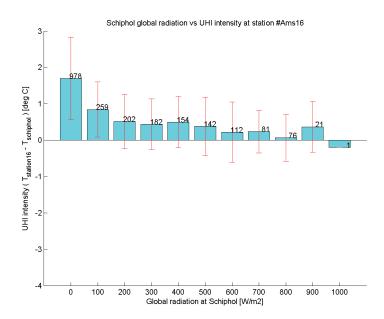
18.35 °C Average temperature Average UHI 1.02 °C Average RH 69.24 % Average dew point temp 12.44 °C Maximum temperature 34.20 °C Recorded at: 19-7-2014 14:00 Minimum temperature 10.30 °C Recorded at: 05-06-2014 04:00 Max UHI 5.4 °C Recorded at: 19-07-2014 20:00 -2.2 °C Min UHI Recorded at: 11-8-2014 12:00 Average unobstructed solar possible using SVF photos: 8.4 hours / day











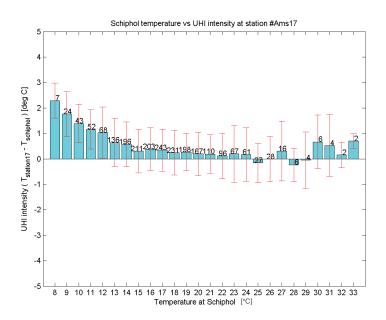


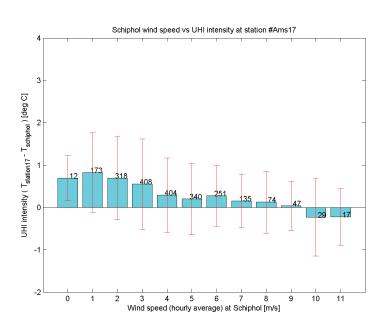
Logger number Latitude Longitude Elevation ASL Sky-view-factor Average NDVI Building presence Building height Vegetation Water Traffic People 2195 N 52.3965 E 4.9579 0.0 m 0.658 0.392 Partly built Normal (10-15m) A few trees Small water body nearby Some No June, July, August:

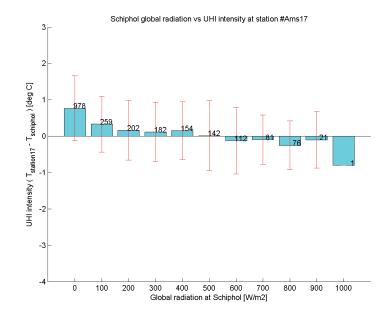
17.73 °C Average temperature Average UHI 0.39 °C Average RH 77.59 % Average dew point temp 13.52 °C Maximum temperature 33.80 °C Recorded at: 19-7-2014 14:00 Minimum temperature 9.50 °C Recorded at: 02-06-2014 04:00 Max UHI 4.4 °C Recorded at: 04-07-2014 02:00 -3.5 °C Min UHI Recorded at: 5-8-2014 15:00 Average unobstructed solar possible using SVF photos: 10.3 hours / day











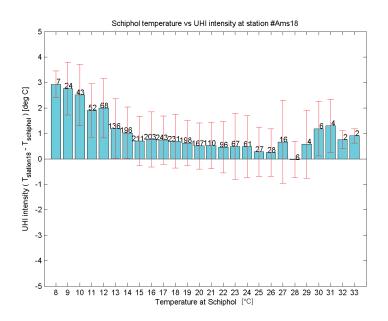


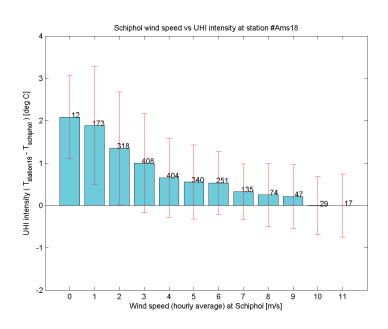
Logger number Latitude Longitude Elevation ASL Sky-view-factor Average NDVI Building presence Building height Vegetation Water Traffic People 2235 N 52.3568 E 4.9157 2.0 m 0.353 0.241 Surrounded by buildings Normal (10-15m) A few trees No No No June, July, August:

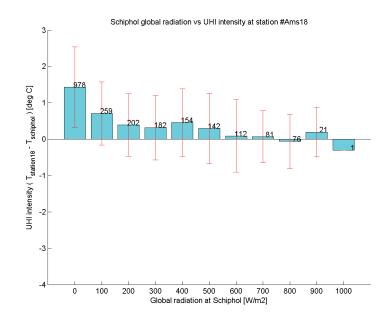
Average temperature	18.17 °C
Average UHI	0.84 °C
Average RH	68.61 %
Average dew point temp	12.08 °C
Maximum temperature	34.00 °C
Recorded at:	19-7-2014 14:00
Minimum temperature	9.90 °C
Recorded at:	05-06-2014 04:00
Max UHI	5.4 °C
Recorded at:	19-07-2014 20:00
Min UHI	-2.9 °C
Recorded at:	23-8-2014 9:00
Average unobstructed solar	
possible using SVF photos:	8.2 hours / day











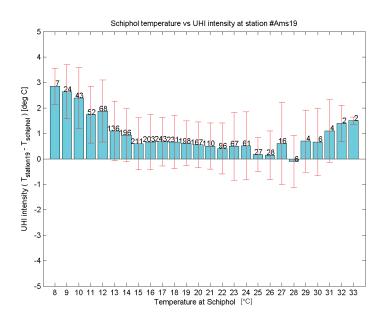


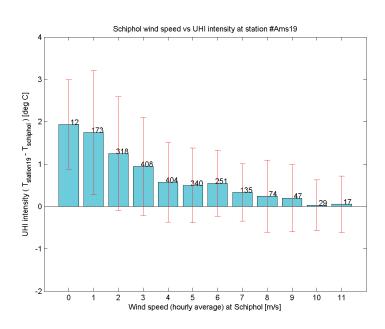
Logger number Latitude Longitude Elevation ASL Sky-view-factor Average NDVI Building presence Building height Vegetation Water Traffic People 2231 N 52.3632 E 4.9383 2.0 m 0.354 0.280 Surrounded by buildings High (15-20m) A few trees No No Some June, July, August:

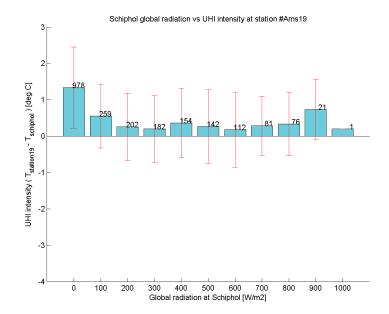
18.11 °C Average temperature Average UHI 0.78 °C Average RH 70.53 % Average dew point temp 12.46 °C Maximum temperature 34.70 °C Recorded at: 19-7-2014 14:00 Minimum temperature 9.80 °C Recorded at: 05-06-2014 04:00 Max UHI 5.5 °C Recorded at: 19-07-2014 20:00 -2.7 °C Min UHI Recorded at: 23-8-2014 9:00 Average unobstructed solar possible using SVF photos: 6.9 hours / day













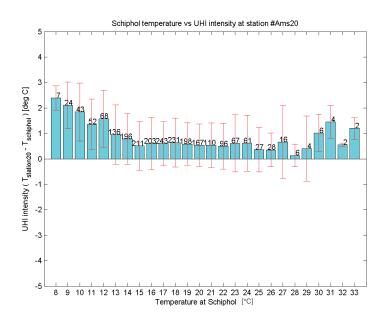
Logger number Latitude Longitude Elevation ASL Sky-view-factor Average NDVI Building presence Building height Vegetation Water Traffic People 2237 N 52.3493 E 4.8699 1.0 m 0.353 0.353 Surrounded by buildings Normal (10-15m) Trees every few metres No Some No

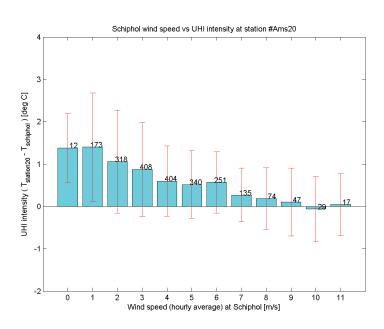
## June, July, August:

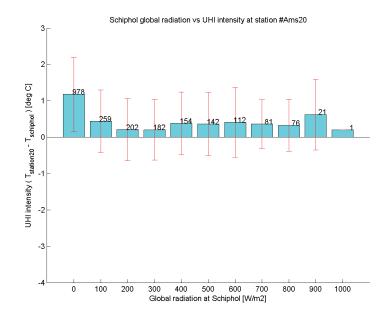
18.04 °C Average temperature Average UHI 0.71 °C Average RH 69.89 % Average dew point temp 12.24 °C Maximum temperature 34.20 °C Recorded at: 19-7-2014 14:00 Minimum temperature 9.90 °C Recorded at: 05-06-2014 04:00 Max UHI 6.0 °C Recorded at: 18-07-2014 20:00 -2.6 °C Min UHI Recorded at: 18-8-2014 12:00 Average unobstructed solar possible using SVF photos: 4.9 hours / day













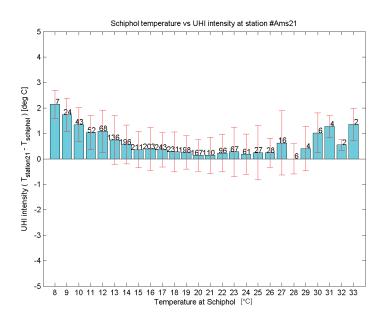
Logger number Latitude Longitude Elevation ASL Sky-view-factor Average NDVI Building presence Building height Vegetation Water Traffic People 2239 N 52.3554 E 4.7838 -3.0 m 0.728 0.296 Partly built Normal (10-15m) A few trees No No No

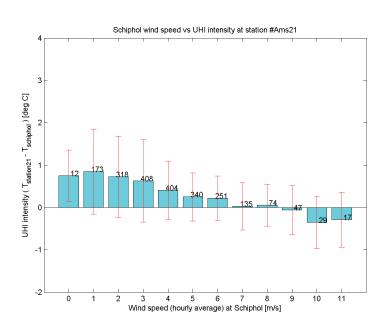
## June, July, August:

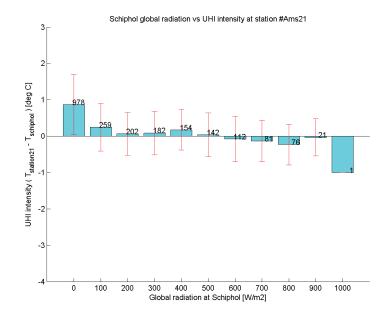
17.75 °C Average temperature Average UHI 0.42 °C Average RH 69.03 % Average dew point temp 11.77 °C Maximum temperature 34.30 °C Recorded at: 19-7-2014 13:00 Minimum temperature 9.70 °C Recorded at: 21-08-2014 05:00 Max UHI 6.2 °C Recorded at: 18-07-2014 20:00 -2.5 °C Min UHI Recorded at: 18-8-2014 11:00 Average unobstructed solar possible using SVF photos: 11.6 hours / day











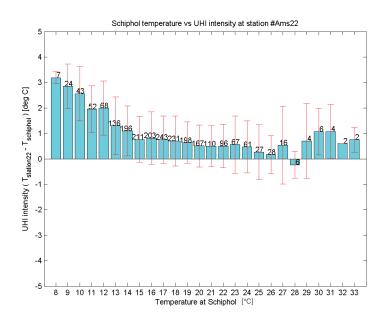


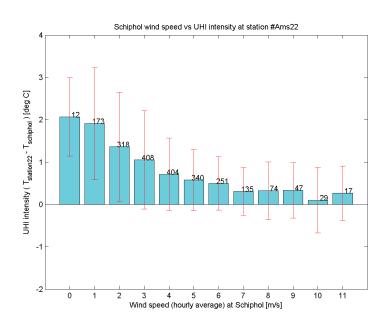
Logger number Latitude Longitude Elevation ASL Sky-view-factor Average NDVI Building presence Building height Vegetation Water Traffic People 2225 N 52.3667 E 4.8705 3.0 m 0.644 0.241 Surrounded by buildings High (15-20m) A few trees Small water body nearby Normal Crowded June, July, August:

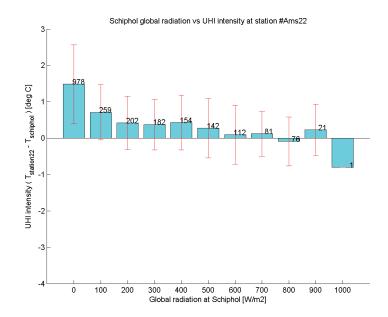
18.20 °C Average temperature Average UHI 0.87 °C Average RH 72.34 % Average dew point temp 12.90 °C Maximum temperature 33.70 °C Recorded at: 19-7-2014 14:00 Minimum temperature 10.20 °C Recorded at: 05-06-2014 04:00 Max UHI 6.1 °C Recorded at: 18-07-2014 20:00 -2.3 °C Min UHI Recorded at: 11-8-2014 12:00 Average unobstructed solar possible using SVF photos: 10.6 hours / day











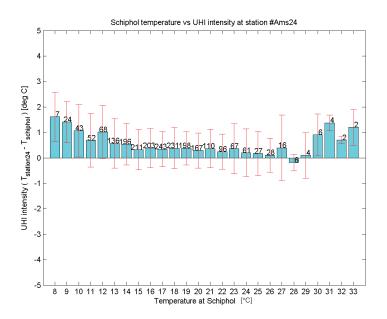


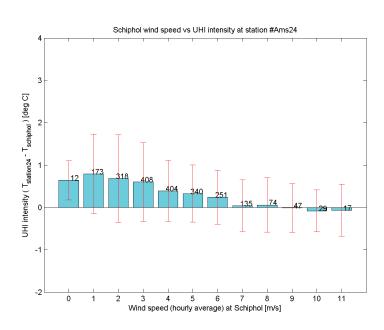
Logger number Latitude Longitude Elevation ASL Sky-view-factor Average NDVI Building presence Building height Vegetation Water Traffic People 2199 N 52.3173 E 4.8780 -2.0 m 0.750 0.394 Surrounded by buildings High (15-20m) A few trees Small water body nearby Normal Some June, July, August:

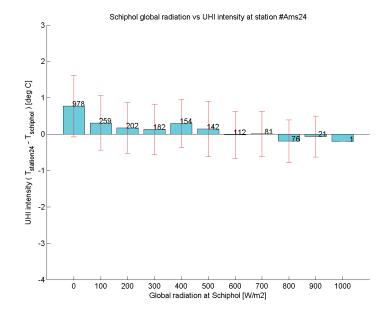
17.76 °C Average temperature Average UHI 0.43 °C Average RH 71.57 % Average dew point temp 12.29 °C Maximum temperature 34.20 °C Recorded at: 19-7-2014 13:00 Minimum temperature 8.40 °C Recorded at: 06-06-2014 04:00 Max UHI 5.1 °C Recorded at: 18-07-2014 20:00 -3.0 °C Min UHI Recorded at: 17-8-2014 22:00 Average unobstructed solar possible using SVF photos: 13.6 hours / day













- Logger number Latitude Longitude Elevation ASL Sky-view-factor Average NDVI Building presence Building height Vegetation Water Traffic People
- 2240 N E 0.0 m 0.296 Surrounded by buildings Very high (>20m) A few trees No Normal Crowded

June, July, August:

Average temperature Average UHI Average RH Average dew point temp Maximum temperature Recorded at: Minimum temperature Recorded at: Max UHI Recorded at: Min UHI Recorded at: Average unobstructed solar possible using SVF photos:

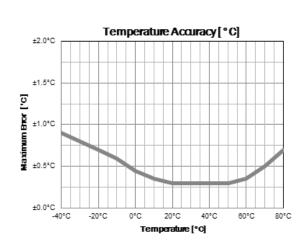
No observations in this period due to a disconnected data logger.





р. 97

VP-3 temperature/humidity sensor from	Decagon Devices:
HUMIDITY RESOLUTION:	0.1% RH
TEMPERATURE RESOLUTION:	0.1°C
VAPOR PRESSURE RESOLUTION:	0.01 kPa
HUMIDITY RANGE:	0-100% RH
TEMPERATURE RANGE:	-40°C to 80°C
VAPOR PRESSURE RANGE:	0-47 kPa
SENSOR TYPE:	Digital Capacitance and Thermistor
OUTPUT:	RS232, SDI-12
OPERATING ENVIRONMENT:	-40°C to 80°C
CABLE LENGTH:	5 m
CABLE CONNECTOR TYPES:	3.5 mm "stereo" plug or three-wire
POWER REQUIREMENTS:	3.6-15 VDC, 0.03 mA quiescent, 4 mA during 300 ms measurement
SENSOR DIMENSIONS:	5.4 cm x 1.96 cm
RADIATION SHIELD DIMENSIONS:	8.9 cm height, 10.16 cm diameter, 13.34 cm wide (bracket)
DATA LOGGER COMPATIBILITY (NOT EXCLUSIVE):	Decagon Em50 series (firmware 2.11 or newer), ProCheck C (Rev 1.5), Campbell Scientific



				Humi	dity /	Accur	acy [	%RH	]	
	100%	±5%	±5%	±5%	±5%	±5%	±5%	±5%	±6%	±10%
	95%	±5%	±5%	±4%	±4%	±4%	±4%	±4%	±5%	±8%
	90%	±5%	±4%	±2%	±2%	±3%	±3%	±4%	±5%	±8%
	85%	±5%	±4%	±2%	±2%	±3%	±3%	±4%	±5%	±8%
	80%	±4%	±4%	12%	12%	±3%	±3%	±3%	±4%	±6%
	75%	±4%	±4%	±2%	±2%	±3%	±3%	±3%	±4%	±6%
100000	70%	±4%	±4%	±2%	±2%	±3%	±3%	±3%	±4%	±6%
Ξ	65%	±4%	±4%	±2%	±2%	±3%	±3%	±3%	±4%	±6%
[%RH]	60%	±4%	±3%	±2%	±2%	±2%	±2%	±2%	±3%	±5%
	55%	±4%	±2%	±2%	±2%	±2%	±2%	±2%	±3%	±5%
Humidity	50%	±4%	±2%	±2%	±2%	±2%	±2%	±2%	±3%	±5%
2	45%	±4%	±2%	±2%	±2%	±2%	±2%	±2%	±3%	±4%
	40%	±4%	±2%	±2%	±2%	±2%	±2%	±2%	±3%	±4%
Ŧ	35%	±4%	±3%	±2%	±2%	±2%	±2%	±2%	±3%	±4%
	30%	±4%	±3%	±2%	12%	±2%	±2%	±2%	±3%	±4%
	25%	±4%	±3%	±2%	±2%	±2%	±2%	±2%	±3%	±4%
	20%	±4%	±4%	±2%	:2%	±3%	±3%	±3%	±3%	±4%
	15%	±5%	±4%	±2%	±2%	±3%	±3%	±4%	±4%	±5%
	10%	±8%	±5%	±3%	±3%	±4%	±4%	±4%	±5%	±8%
	5%	±8%	±8%	±5%	±5%	±5%	±5%	±5%	±6%	±10%
	0%	±12%	±12%	±5%	±5%	±6%	±6%	±6%	±10%	±12%
		0°C	10°C	20°C	30°C	40°C	50°C	60°C	70°C	80°C
	8				Temp	eratur	e [°C]			

# DS-2 Sonic anemometer from Decagon Devices:

WIND SPEED RANGE:	0 to 30 m/s
WIND SPEED RESOLUTION:	0.01 m/s
WIND SPEED ACCURACY:	0.30 m/s or < 3%, whichever is larger
WIND DIRECTION RANGE:	0 to 359 degrees
WIND DIRECTION RESOLUTION:	1 degree
WIND DIRECTION ACCURACY:	±3 degrees
OPERATING TEMPERATURE RANGE:	-40 to 50 C
EXCITATION VOLTAGE:	3.6 to 15 VDC
CURRENT:	0.03 mA quiescent, 0.5 mA sampling, < 0.05 mA average
DATA LOGGER COMPATIBILITY (NOT EXCLUSIVE):	Decagon Em50 Series, ProCheck, Campbell Scientific
	Decagon Em50 Series, ProCheck, Campbell Scientific
EXCLUSIVE):	100 mm
EXCLUSIVE): DIAMETER:	100 mm 75 mm
EXCLUSIVE): DIAMETER: HEIGHT (WIND SENSOR):	100 mm 75 mm 155 mm
EXCLUSIVE): DIAMETER: HEIGHT (WIND SENSOR): HEIGHT (TOTAL W/ MOUNT):	100 mm 75 mm 155 mm
EXCLUSIVE): DIAMETER: HEIGHT (WIND SENSOR): HEIGHT (TOTAL W/ MOUNT): MAXIMUM SAMPLING SPEED1:	100 mm 75 mm 155 mm 1 Hz

<sup>1</sup>If sampling rate is greater than 0.1 Hz, the anemometer reports the speed and direction at the time of sampling. If sampled less frequently, the anemometer samples every 10 seconds, averages the vector components of the wind, and keeps the maximum gust. When the logger samples, the anemometer reports the average wind speed, direction, and the maximum gust speed.

# APPENDIX C: DATA SYNCHRONISATION USING TYPICAL WEATHER EVENTS

These pages describe the synchronisation of the data of the 24 stations. Time stamps were distorted at certain times due to connecting the loggers with external equipment. There are 24 stations with 5 minute data time stamps. All starting at the end of May 2014 and in UTC+2. However, during maintenance or manual data collections at the stations, time stamps were sometimes perturbed to local time (UTC, UTC+1 or UTC+2 depending on winter/summer). Using field logs and 2 distinctive weather events the data could be synchronized again. Most stations were visited on October 17th to replace batteries or add extra measuring equipment. On November 2nd, station 2222 was visited. On January 13 and 14, some batteries were replaced.

# **October Front**

As a first check, the front passage of October 7th was used. Around 12.30 UTC+2, a cold front passed over Amsterdam, with a temperature drop of 1 degree in 5 minutes recorded at the stations. The time of the maximum dT was used. As a check, this time was plotted against the longitude. The stations in the west recorded the passage about 20 minutes earlier than those in the east.

# **October battery**

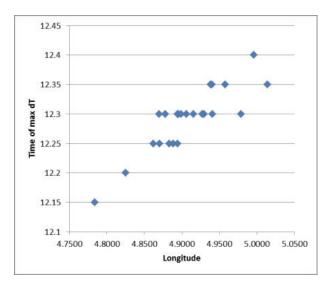
At October 17th, the following stations were visited: 2194, 2221, 2198, 2235, 2238, 2230, 2229, 2245 and 2239. In these stations, a large jump in temperature indicates the moment where the station was connected to the laptop and time changed. Stations 2247, 2223 were also visited but no data jump could be found! 2240 was visited but had no previous data.

# January battery

At January 13th and 14th, the following stations were visited and data jumps were found in 2195, 2226, 2246 and 2231. Station 2240 was visited, but was already UTC. Stations 2199, 2228 and 2241 were visited but no jump was found. Station 2225 was not visited (according to data header) but a data jump was found!

# **January Front**

At January 28th, a strong cold front passed Amsterdam again. All stations except 2223 and 2236 record this passage around 2:40 UTC, indicating that they have changed time stamp sometime since the passage of the October front. 2236 records the passage at 4:40. This station has not been attached to the laptop, and therefor is still in local summer time. Station 2223 was connected, but records the passage at 3:40. This could be caused by the fact that it was winter time when the station was connected, in contrast to summer time.





The Urban Heat Island effect of Amsterdam: observations and models in 2014 and projections of the future urban climate.

MSc Thesis Willem van der Pas

Wageningen University 2015